Sudan University for science and technology

College of Engineering

Biomedical Engineering Department

Mathematical Modeling of Light-Malaria Blood interaction using Monte Carlo Simulation

Prepared by:

Aisha Alfaki Mohamad

Malaz Taha Mohammed

Zainab Ragab Mohammed

Supervised by:

T.Ola Salahaldein

October 2017

الآيــة

"إقـرا بـاسم ربـك الـذي خلق، خلق الانـسـان من علق، إقـرا وربـك الاكـرم، الـذي علم بـالـقـلم، علم الانـسـان مـا لـم يـعـلم"

صدق الله الـعظيم

سورة الـعلق

Dedication

I do not like the night except with your thankfulness and do not like the day except by your obedience

God is great

To whom the message reached the Valley of the Secretariat ... And advise the nation ... to the prophet of mercy ... And the world

Prophet Mohammed peace be upon him

To those whom God has shown with honor and glory ... to those who taught me tenderness without waiting ... to whom I carry his name with all pride ... and ask God to extend in your age to show fruit that has come to be harvested after a long wait ... and I will keep your words stars, guided today, tomorrow and forever. ..

Dearest Father

To my angel in life ... To the meaning of love and to the meaning of compassion and dedication

To whom was the secret of my success to the most expensive Habayeb ……

Beloved Mother

Who are my Sindi and my strength and my refuge after God to those who impressed me on themselves to those who taught me the meaning of life to love , my heart and my destiny.....

My brothers

To the comrades of science and the path…….

My colleagues and brothers in the study

To all those who added to the outcome of my knowledge of the characters all of them dedicate this research .

Acknowledgements

All thanks to Allah Almighty who gave us the strength, Determination, health and granted us with patience to successfully complete of this research.
we cannot express enough thanks to our supervisor **T. Ola Salah Eldien** for her continued guidance, support, unlimited helps and encouragement .
Our completion of this research could not have been accomplished without the support of our **parents**. Our deepest gratitude, special appreciation and thanks to:

Dr. Sharif Fadul Babiker who guide us to complete our research and help to implement program simulation may Alla bless him ,and thanks to bio medical engineering teachers ,our college, our family ,our colleagues and friends and every person help and support us.

Contents

List of figures

Abbreviations

Plasmodium	P
World Health Organization	who
Gram per deciliter	gm/dl
Haemoglobin	H b
red blood cells	RBCs
White blood cells	WBCs
platelets	PLTs
Infra-Red	IR
ultraviolet	UV
nanometer	nm
Random number	RND
centimeter	cm
absorption coefficient	µa
scattering coefficient	µs
total attenuation	µt
Light Amplification by Stimulated Emission of Radiation	Laser
Wavelength	ʎ
Degree	°
montecarlo multilayer	mcml
Radial position	r

Fluence rate of spherical	Fsph
Fluence rate of cylindrical	Fcyl
Fluence rate of planar	Fpla

Abstract

The laser treatment in medical field has become popular. While interacting of laser with tissue, photons experience refraction, reflection, absorption and scattering, getting uniform distributed in the tissue depending upon random distribution and optical parameters and properties of tissue. This research focus on using the light interaction with tissue in this case Blood tissue to determine presence of malaria parasite . The distribution of photon is simulated effectively by using Monte Carlo method. The study showed that the photon distribution is affected by the tissue parameters and light parameters. Depend on the result that Monte Carlo showed the different between the interactions with normal and abnormal blood is obtained and they are using in determine the presence of malaria parasite.

المستخلص

أصبح العلاج والتشخيص باستخدام الليزر في المجالات الطبية أكثر انتشارا في الآونة الأخيرة. في تفاعلات الليزر مع الانسجة نجد ان الفوتونات يحدث لها الانكسار،الانعكاس،الامتصاص والتشتت،والحصول على توزيع موحد في الأنسجة اعتمادا على التوزيع العشوائي والمعاملات البصرية وخصائص الأنسجة. يركز هذا البحث علي استخدام تفاعلات الضوء(الفوتون) مع الدم في تحديد وجود طفيل الملاريا في الدم . ويتم محاكاة توزيع الفوتون بشكل فعال باستخدام طريقة مونت كارلو. وأظهرت الدراسة أن توزيع الفوتون يتأثر بمعاملات الأنسجة ومعاملات الضوء نفسه .واعتمادا علي النتيجة التي يظهرها المونت كارلو يتم فحص التباين في تفاعلات الضوء مع الدم السليم وتفاعلاته مع دم المريض بالملاريا لتحديد وجود المرض من خلال تغير يطرأ في شكل وتركيب عينة الدم .

Chapter one

Introduction

1.1General Overview

Malaria is caused by infection with protozoan parasites belonging to the genus plasmodium transmitted by female anopheles species mosquitoes .Our understanding of the malaria parasites begins in 1880 with the discovery of the parasites in the blood of malaria patients by Alphonselaveran
The sexual stages in the blood were discovered by William MacCallum in birds infected with a related haematozoan , Haemoproteus columbae ,in 1897and the whole of the transmission cycle in culicine mosquitoes and birds infected with plasmodium relictum was elucidateted by Ronald Ross in 1897.
In 1898 the Italian malariologists , Giovanni Basttista Grassi,Amico Bignami, Giuseppe Bastianelli ,Angelo Celli ,camillo Golgi and Ettore Marchiafava demonstrated conclusively that human malaria was also transmitted by mosquitoes, in this case anophelines.The discovery that malaria parasites developed in the liver before entering the blood stream was made by Henry Shortt and Cyril Garnham in 1948 and the final stage in the life cycle ,thepresence of dormant stages in the liver ,was conclusively demonstrated in 1982 by Wojciech Krotoski[1].

In this research new method was developing to detect malaria mainly depend on how the light interaction with blood. When blood are exposed to light reflection ,refraction ,absorption ,or scattering can occur ,which lead to energy losses in the incident beam. Reflection is defined as the returning of electromagnetic radiation by surfaces upon which it is incident. In general, a reflecting surface is the physical boundary between two materials of different indices of refraction such as air and tissue[2].

During absorption, the intensity of an incident electromagnetic wave is attenuated in passing through a medium. The absorbance of a medium is defined as the ratio of absorbed and incident intensities. Absorption is due to a partial conversion of light energy into heat motion or certain vibrations of molecules of the absorbing material[2].

When elastically bound charged particles are exposed to electromagnetic waves, the particles are set into motion by the electric field. If the frequency of the wave equals the natural frequency of free vibrations of a particle, resonance occurs being accompanied by a considerable amount of absorption[2].

1.2 PROBLEM STATEMENT

The traditional methods of diagnosing malaria depend mainly on the skills of the laboratory technicians, and take long time . Therefore, it may be inaccurate.

Optical methods can represent a proper solution for the problem and modeling can provide an approximation for the actual experiment.

1.3 Objective

The objectives of this research are:

1.3.1 General Objectives

TO Determine the optical parameters related to blood malaria using Monte Carlo to model of light tissue interaction.

1.3.2 Specific objectives

The specific objectives of this research are to:

1- Determine the optical parameters of blood compositions and light source.
2- Develop Mathematical modeling and simulation of light-blood interaction.

3- Compare the output results for the normal and malaria infected models to determine the diagnostic parameters.

1.4 Methodology

The methodology depend on three steps:

- First step was studying of interaction of light and malaria blood , light characteristics parameter and equation .
- In second steps was Implementing the equations and parameter in Monte Calro simulation and acquire the Results.
- The third step was evaluation and comparison of the results .

1.5 Thesis layout

The research was divided into six chapters :

Chapter one : Introduction of Malaria , Light tissue interaction , objective problem statement and methodology .

Chapter two : Literature review .

Chapter three : Scientific back ground (Light tissue interaction,Modeling and Monte Carlo).

Chapter four: contained methodology block diagram, calculations of model.

Chapter five: Result and Discussion which discuss an output results.

Chapter six: Conclusion and Recommendations of the research.

Chapter Two

Literature reviews

This chapter discusses the relevant works to this research . It describes the ways that Researchers use to study interaction with light . It provides summery of Some researchers works as it is seen below .

2.1 Simulation of photon propagation in tissue using Matlab

This work investigates the photon transmigration in tissue to noninvasive pulse oximetry measurement of fetal oxygen saturation in maternal abdomen. Simulation is done to three cases and the results are compared to literature. 50000 photons are used in first case and the average absorption is 0.2418. For second case 5000 photons packet are used and average absorption 0.4466 and 0.4310 average absorption for 100000 photon [3].

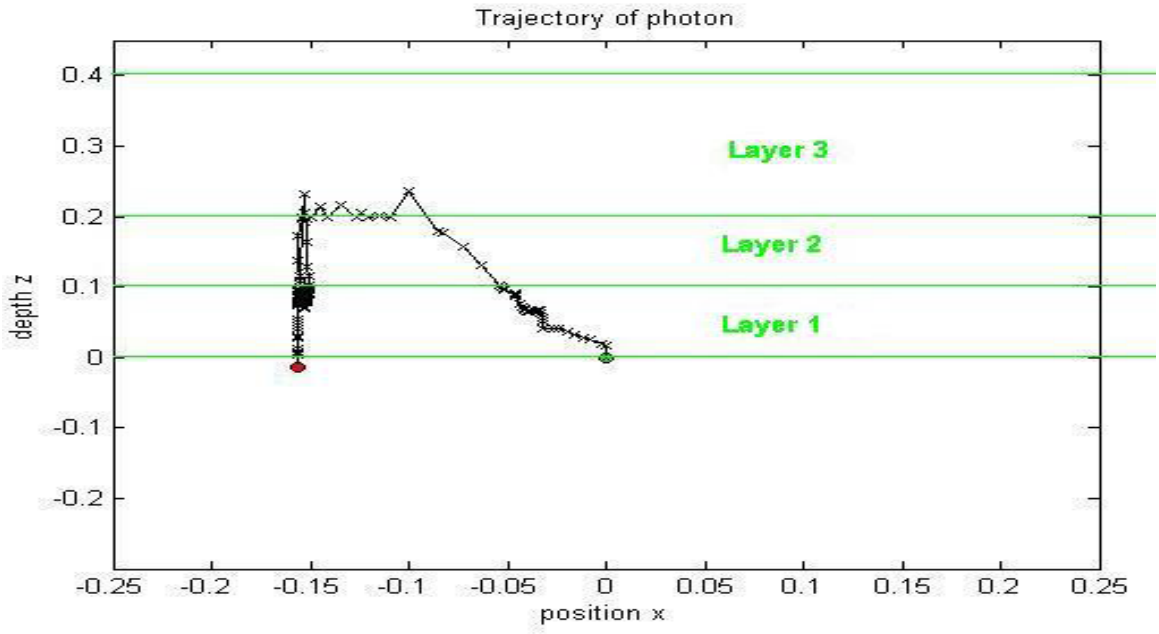

Figure2.1 Trajectory of a single photon in cm (left) and radiation distribution of the single photon (right) It show the photon interaction with the tissue for a single photon. These results are based on the multi-layered tissue simulation[3].

2.2 A Monte Carlo Model of Light Propagation in Tissue

Monte Carlo method was used in this study to discuss photon reflection, absorption and scattering and give method for estimating uncertainty .This study shows that Monte Carlo model allows Calculation of reflection , transmission and fluence rate in tissue .Both mismatched boundary conditions and anisotropic scattering have been included, thereby increasing the realism of the model[4].

2.3 Anew Monte Carlo a new Monte Carlo code for absorption simulation of laser-skin tissue interaction

diode laser in skin tissue .The principal of Monte Carlo was used to create new code with mat lab . The result had been compared with Monte Carlo multilayer code and it proved to have good accuracy.

This study aimed to simulate absorption hair removal[5].

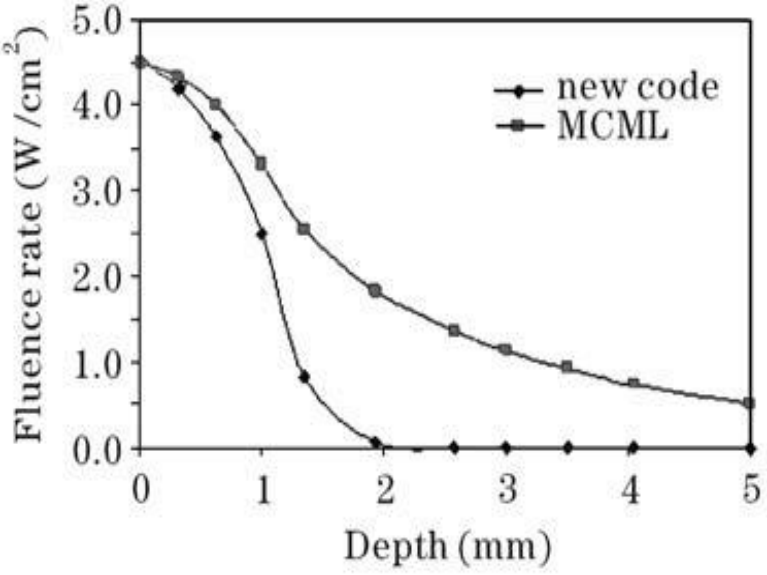

Figure2-2 : shows the result of validating the code by giving the fluence rate distributions in skin depth[5].

2.4 Backward elastic light scattering of malaria infected red blood cells

Since the elastic scattering depends on structure or material characteristics such as size and Chemical composition it was used in this research to diagnosis malaria [22].

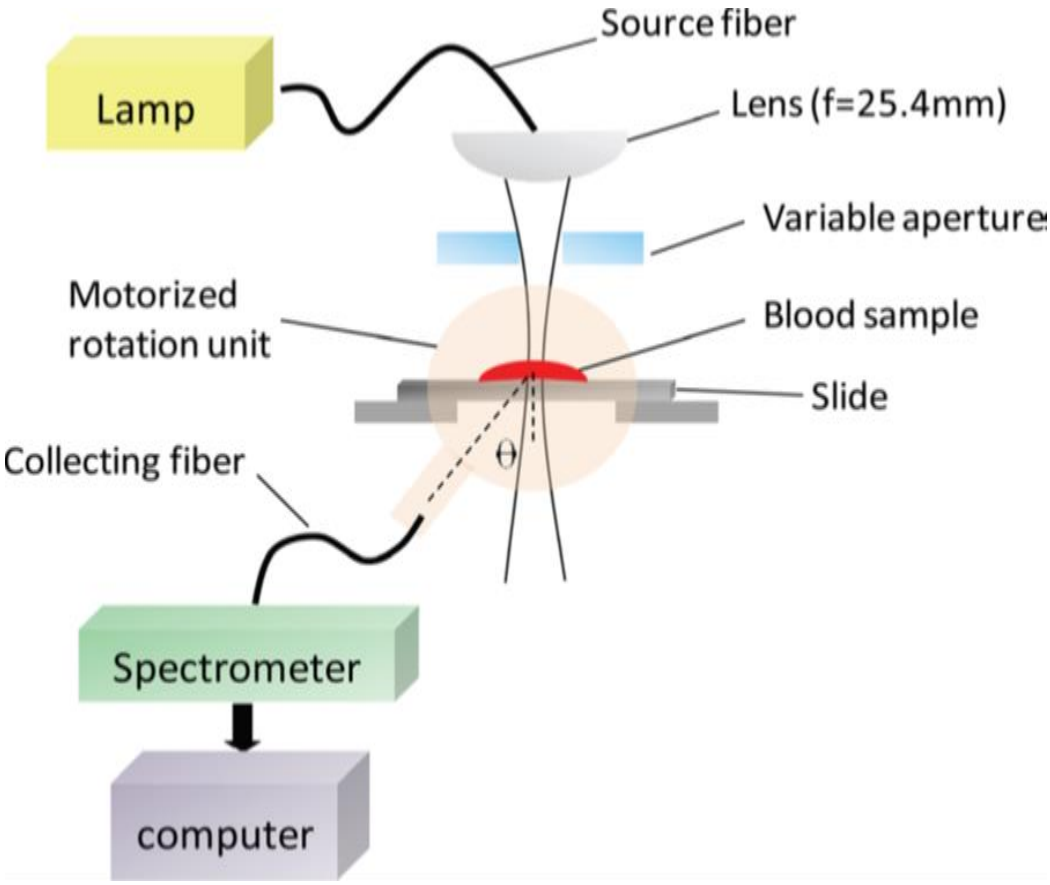

Figure 2-3:Schematic of the optical setup for light scattering measurement[22].

The result had shown difference of infected and non infected blood and suggest the back scattering as potential tool for noninvasive diagnosis.

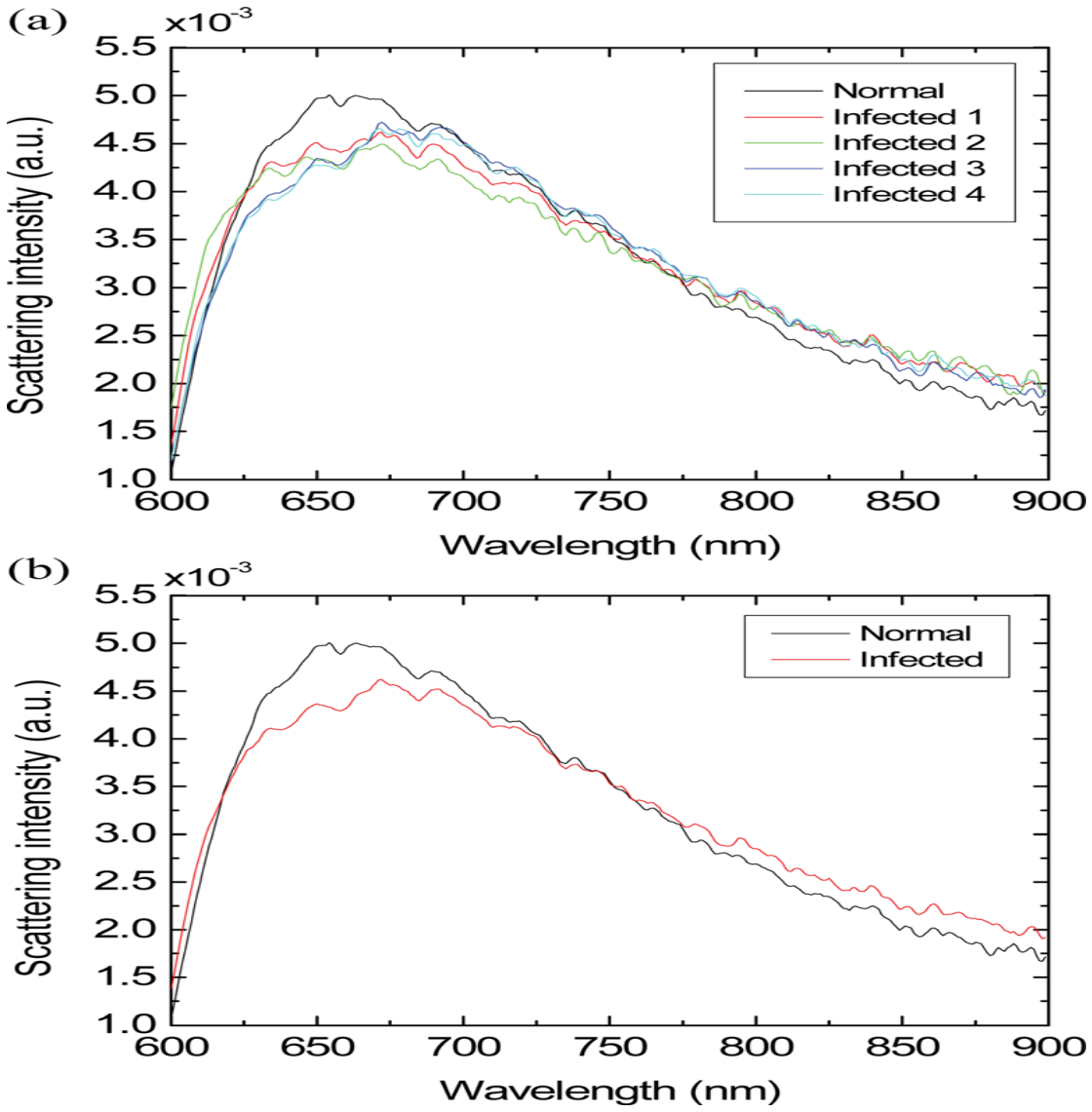

Figure2-4:Backward scattering of healthy and infected sample measured at angle 150[22].

Chapter Three
Theoretical background

3.1 Blood

Define blood as :

Is only fluid tissue in the human body its five more thicker than water and classified as connective tissue and it compound from:

1. **Red cells (erythrocytes)**

These make blood a red color. One drop of blood contains about five million red cells. A constant new supply of red blood cells is needed to replace old cells that break down. Millions of red blood cells are made each day. Red cells contain a chemical called haemoglobin. This binds to oxygen and takes oxygen from the lungs to all parts of the body[6].

Hemoglobin also plays an important role in maintaining the shape of the red blood cells. In their natural shape, red blood cells are round with narrow centers resembling a donut without a hole in the middle. Abnormal hemoglobin structure can, therefore, disrupt the shape of red blood cells and impede their function and flow through blood vessels [7].

2. **White cells (leukocytes)**

There are different types of white cells which are called neutrophils (polymorphs), lymphocytes, eosinophils, monocytes and basophils. They are part of the immune system. Their main role is to defend the body against infection. Neutrophils engulf germs (bacteria) and destroy them with special chemicals. Eosinophils and monocytes also work by swallowing up foreign particles in the body. Basophils help to intensify inflammation. Inflammation makes blood vessels leaky. This

helps specialised white blood cells get to where they are needed. Lymphocytes have a variety of different functions. They attack viruses and other germs (pathogens). They also make antibodies which help to destroy pathogens[6].

3. **Platelets**

These are tiny and help the blood to clot if we cut ourselves[6].

4. **Plasma**

This is the liquid part of blood and makes up about 60% of the blood's volume. Plasma is mainly made from water but also contains many different proteins and other chemicals, such as: (Hormones , Antibodies , Enzymes , Glucose , Fat particles ,Salts.)When blood spills from your body (or a blood sample is taken into a plain glass tube) the cells and certain plasma proteins clump together to form a clot. The remaining clear fluid is called serum[6].

3.2 Life cycle of Malaria

The natural ecology of malaria involves malaria parasites infecting successively two types of hosts: humans and female *Anopheles* mosquitoes. In humans, the parasites grow and multiply first in the liver cells and then in the red cells of the blood. In the blood, successive broods of parasites grow inside the red cells and destroy them, releasing daughter parasites ("merozoites") that continue the cycle by invading other red cells.

The blood stage parasites are those that cause the symptoms of malaria. When certain forms of blood stage parasites ("gametocytes") are picked up by a female *Anopheles* mosquito during a blood meal, they start another, different cycle of growth and multiplication in the mosquito.

After 10-18 days, the parasites are found (as "sporozoites") in the mosquito's salivary glands. When the *Anopheles* mosquito takes a blood meal on another human, the sporozoites are injected with the mosquito's saliva and start another human infection when they parasitize the liver cells.

Thus the mosquito carries the disease from one human to another (acting as a "vector"). Differently from the human host, the mosquito vector does not suffer from the presence of the parasites

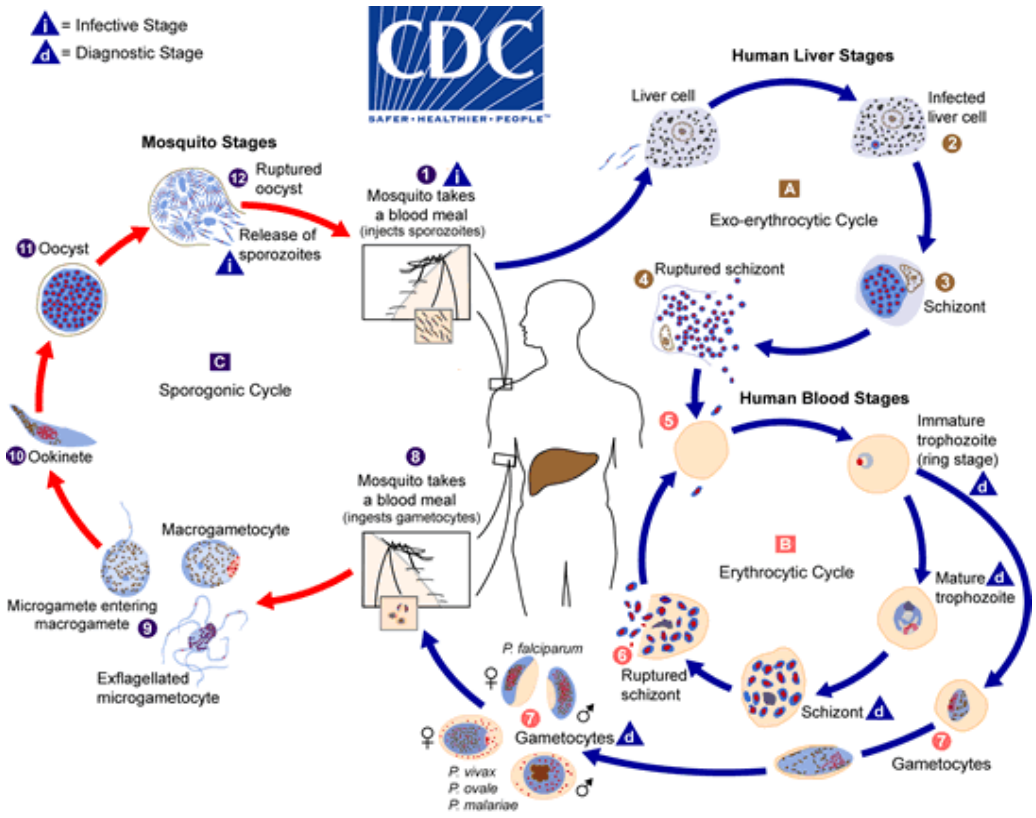

Figure 3-1: Life cycle of malaria parasite[8].

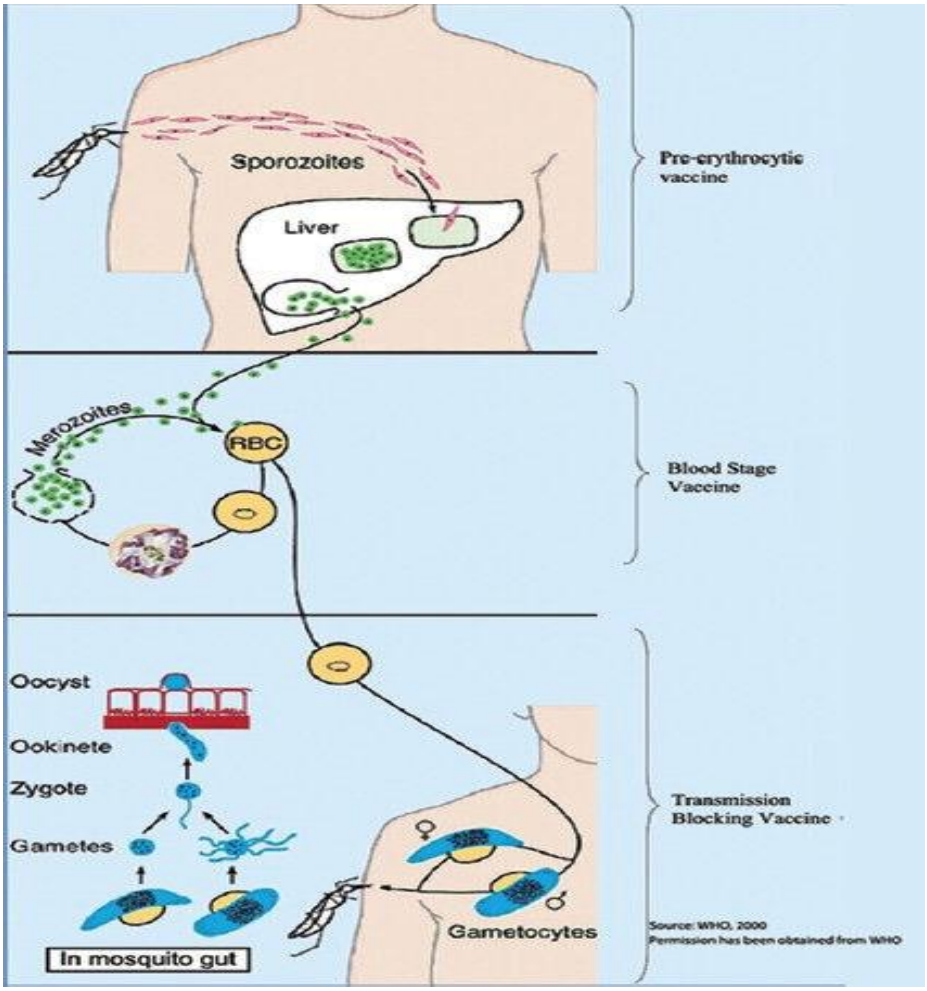

Figure 3-2 : Life cycle of malaria parasite[8].

The malaria parasite life cycle involves two hosts. During a blood meal, a malaria-infected female *Anopheles* mosquito inoculates sporozoites into the human host . Sporozoites infect liver cells and mature into schizonts , which rupture and release merozoites . (Of note, in *P. vivax* and *P. ovale* a dormant stage [hypnozoites] can persist in the liver and cause relapses by invading the bloodstream weeks, or even years later.) After this initial replication in the liver (exo-erythrocytic schizogony A), the parasites undergo asexual multiplication in the erythrocytes (erythrocytic schizogony B). Merozoites infect red blood cells . The ring stage trophozoites mature into schizonts, which rupture releasing merozoites . Some parasites

differentiate into sexual erythrocytic stages (gametocytes) . Blood stage parasites are responsible for the clinical manifestations of the disease.

The gametocytes, male (microgametocytes) and female (macrogametocytes), are ingested by an *Anopheles* mosquito during a blood meal . The parasites' multiplication in the mosquito is known as the sporogonic cycle C. While in the mosquito's stomach, the microgametes penetrate the macrogametes generating zygotes . The zygotes in turn become motile and elongated (ookinetes) which invade the midgut wall of the mosquito where they develop into oocysts . The oocysts grow, rupture, and release sporozoites , which make their way to the mosquito's salivary glands. Inoculation of the sporozoites into a new human host perpetuates the malaria life cycle[8].

3.3 Spread of Malaria

- Malaria is a life-threatening disease caused by parasites that are transmitted to people through the bites of infected female *Anopheles* mosquitoes.
- In 2015, 91 countries and areas had ongoing malaria transmission.
- Malaria is preventable and curable, and increased efforts are dramatically reducing the malaria burden in many places.
- Between 2010 and 2015, malaria incidence among populations at risk (the rate of new cases) fell by 21% globally. In that same period, malaria mortality rates among populations at risk fell by 29% globally among all age groups, and by 35% among children under 5.
- The WHO African Region carries a disproportionately high share of the global malaria burden. In 2015, the region was home to 90% of malaria cases and 92% of malaria deaths[9].

Malaria occurs mostly in poor, tropical and subtropical areas of the world

Africa is the most affected due to a combination of factors:

- A very efficient mosquito (*Anopheles gambiae* complex) is responsible for high transmission.
- The predominant parasite species is *Plasmodium falciparum*, which is the species that is most likely to cause severe malaria and death.
- Local weather conditions often allow transmission to occur year round.
- Scarce resources and socio-economic instability have hindered efficient malaria control activities.

In other areas of the world malaria is a less prominent cause of deaths, but can cause substantial disease and incapacitation, especially in rural areas of some countries in South America and South Asia[10].

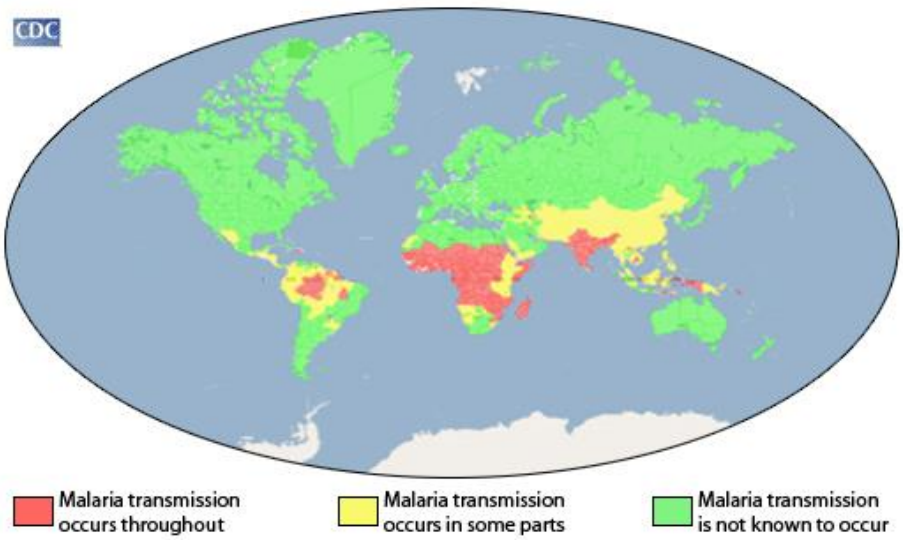

Figure3-3:Malaria on world[10].

3.4 Malaria types

The four types of Plasmodium is Plasmodium falciparum ,Plasmodium malariae, Plasmodium vivax. and Plasmodium ovale. The most popular type spread among the world is: Plasmodium falciparum Which is responsible for most malaria deaths, especially in Africa. The infection can develop suddenly and produce several life-threatening complications. With prompt, effective treatment, however, it is almost always curable[11].

3.5 Effects of malaria parasite on blood

During infection, malarial parasites invade erythrocytes and digest the protein (globin) part of the hemoglobin molecule. The heme component, which is toxic to the parasite, is converted into insoluble hemozoin in the form of rodlike crystals; the transformation of low-spin (Fe^{+2}) diamagnetic oxyhemoglobin into high-spin (Fe^{+3}) paramagnetic hemozoin produces a change in magnetic state of blood[12].

Invasion by the malaria parasite, P. falciparum (the most severe form of malaria) brings about extensive changes in the host red cells. These include loss of the normal discoid shape, increased rigidity of the membrane, elevated permeability to a wide variety of ionic and other species, and increased adhesiveness, most notably to endothelial surfaces[13].

A protein called RESA that causes cell membranes to stiffen within 24 hours of infection. This rigidity impairs the ability of a red blood cell to travel through blood vessels[14].

These effects facilitate survival of the parasite within the host cell and tend to increase the virulence of disease that include cerebral malaria and anemia. Numerous proteins secreted by the internalized parasite and interaction with red cell membrane proteins are responsible for the changes occurring to the host cell.

Anemia a serious clinical manifestation of malaria is due to increased destruction of both infected and uninfected red cells due to membrane alterations, as well as ineffective erythropoiesis[14].

Effect of malarial parasitic infection on blood cells was studied on 809 blood smear diagnosed cases of malaria in a tertiary care hospital.

Muhammad Idris et al.[6] from Abbottabad, Pakistan, reported on 1994 patients out of 145 (7.2%) patients were found infected to malaria.

S. Sahar et al.[7] from Muzaffargarh district, Punjab-Pakistan, reported on 10,028 suspected malaria cases, of which, 208 (2.07%) were confirmed as P. falciparum patients.

Effect of malarial infection on Haemoglobin (Hb) levels, low values of Hb were found consistently with Plasmodium falciparum as compared to Plasmodium vivax. More number of Plasmodium falciparum cases showed low levels of Hb in the range of < 9 gm/dl to 12 gm/dl[15] .

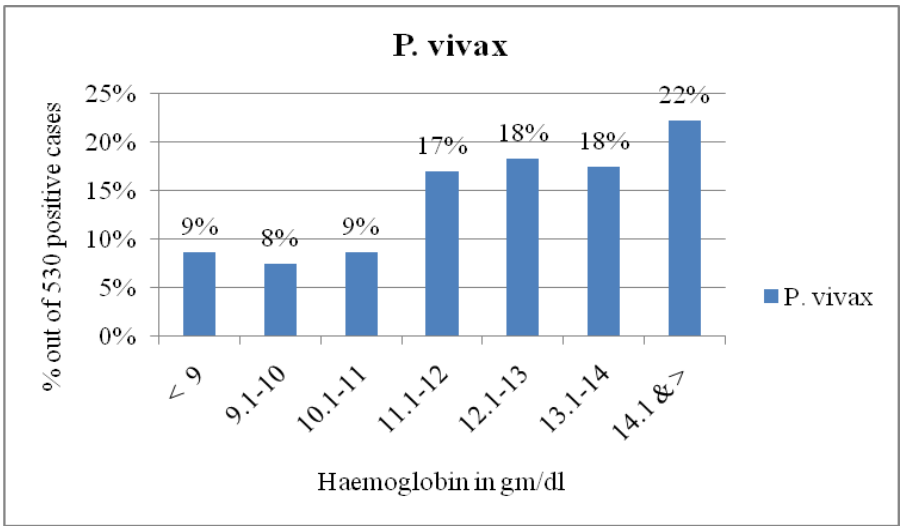

Figure 3-3: Effects of plasmodium vivax on haemoglobin[15].

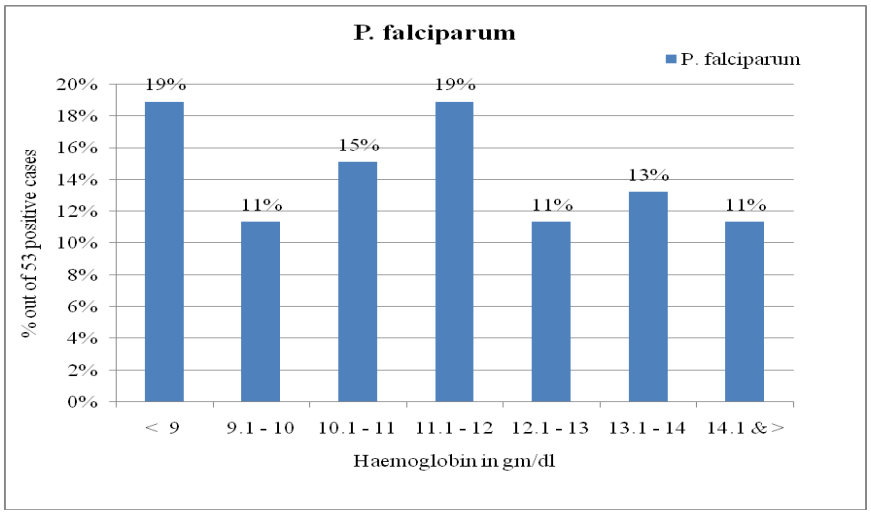

Figure 3-4:Effects of plasmodium falciparum on haemoglobin[15].

3.6 Blood Optical Properties

The cellular portion of blood is called formed elements, and it includes the erythrocytes or red blood cells (RBCs), the white blood cells (WBCs) and the platelets (PLTs). Although the volume fraction of human blood occupied by the formed elements.

The optical properties of human blood under normal physiological conditions are largely determined by light interactions with plasma and RBCs , which account for 99% of the formed elements . The effects of the optical properties of WBCs and PLTs on the light scattering and absorption by whole blood are considered negligible.

RBCs have a thin plasma membrane that encloses mainly a hemoglobin solution. The absorption and scattering of light by the RBCs are two to three orders of magnitude higher than those of the other blood components . The light scattered by a single RBC depends on its shape, volume, refractive index and orientation[16].

3.7 Light interaction with blood

The most important mathematical approaches for modeling the light transport in blood and their domain of application :"The first –order scattering," "monte carlo simulation," "inverse adding –doubling," and "finite element method ".

When blood are exposed to light reflection ,refraction ,absorption ,or scattering can occur, which lead to energy losses in the incident beam.

Refraction is not significant in biomedical applications ,except for laser irradiation of transparent media ,such as cornea tissue ; in opaque media the most important phenomena are scattering and absorption , depending on the material type of the tissue and the incident wavelength.

knowledge of absorbing and scattering properties of the tissue is needed for predicting success of laser surgery treatment .

Direct measurement methods simply use the Beer attenuation law ,but Need corrections when surface reflections occur due to the mismatched refractive indexes.

In direct techniques use theoretical models for the scattering phenomena ; the indirect non iterative methods need simple equations to connect optical properties to measured quantities.

3.7.1 Basic phenomena regarding light and blood

Reflection means the electromagnetic waves return from surfaces upon they are incident. The simple law of reflection states that the reflection angle equals the incidence angle.

The real tissues do not act like optical mirrors ; the roughness of the reflecting surface leads to multiple beam reflection (diffuse reflection).

Refraction means a displacement of the transmitted beam through the surface that separates two media with different refractive indexes ,it is occur together reflection.

The reflectance is the ratio of the reflected and incident intensities , it is equal to the square of the reflectivity.

Absorption means that the incident beam intensity decreases when passing through the tissue, because the beam energy is partly converted into heat motion or into vibration of the absorbent medium molecules.

Absorption in biological tissues is mainly determined by the water molecules ,especially in the IR region of the spectrum and by protein and pigments in the UV and visible range ; melanin is the basic pigment of the skin and hemoglobin is component of vascularized tissue .

Most bio molecules have complex absorption band structures in the 400-600nm range but the spectral range of 600-1200nm(the therapeutic window) is free of absorption phenomena ; neither water nor macromolecules absorb near IR ,so that the light penetrates biological tissues with little loss and enables treatments of profound structures .

Scattering can be elastic (when the incident photon energy has the same value as the scattered photon energy) or inelastic (when a fraction of the incident photon energy is converted into forced vibrations of the medium particles).

Rayleigh scattering is of elastic type ,where the scattering coefficient decreases with fourth power of the wavelength[2].

Light scattering is a well –established experimental technique , which gains more and more popularity in the bio logical field because it offers means for non-invasive imaging and detection.

Light scattering is commonly used in the fields of condensed , soft, and bio logical matter to investigate the structure and dynamics of different constituents within a material sample[17].

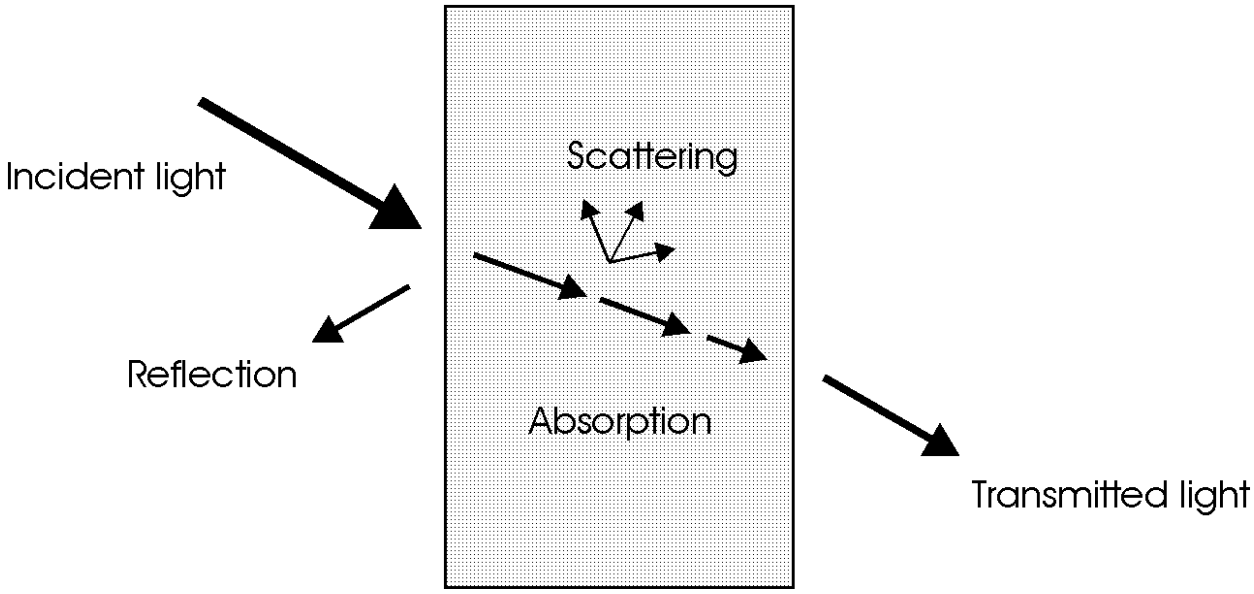

Figure 3-5: Geometry of reflection, refraction, absorption, and scattering[19].

3.7.2 light propagation in blood:

Mathematical description of absorption and scattering can be in two ways .The most fundamental approach is the analytical theory based on Maxwell 's equations ,but their complexity and the in homogeneities of bio logical tissues limit the possibility to obtain the exact analytical solutions thus limiting the applicability of the theory.

The second approach is the photon transport theory , which deals with photon beams passing through absorbing and scattering media , without considering Maxwell's equations ; it was extensively used for laser –tissue interactions where it is predictions were satisfactory in many cases , though it is a less strict theory compared to analytical theories[2].

3.7.3 Mechanisms of Laser-blood Interactions

the most common interaction mechanisms for therapeutic and surgical applications will be divided into five broad classes:

1. In photochemical interactions, photons excite molecules or atoms, making the molecules more likely to undergo chemical reactions with other molecules. In photodynamic therapy ,for instance, a photo sensitiser (a molecule that becomes reactive when it absorbs light and can therefore induce chemical reactions within other molecules or tissue) causes reactive oxygen species to form which lead to both necrosis (cell death) and apoptosis ('programmed' cell death). Photodynamic therapy is increasingly widely used in oncology to destroy cancerous tumours.

2. In photothermal interactions, photons are absorbed by a chromphore (a light-absorbing molecule) and converted into heat energy, which can cause a range of thermal effects from tissue coagulation to vaporization. Applications include tissue cutting and welding in laser surgery.

3. In photoablation, high-energy, ultraviolet (UV) photons are absorbed and, because they are more energetic than the chemical bonds holding the molecules together, cause the dissociation of the molecules. This is followed by rapid expansion of the irradiated volume and ejection of the tissue from the surface. This is used in eye (corneal) surgery, among other applications.

4. In plasma-induced photoablation a free electron is accelerated by the intense electric field in the vicinity of the laser beam. By colliding with a molecule and freeing another electron, it initiates a chain reaction of similar collisions, resulting in a plasma: a soup of ions and free electrons. One application of this is in lens capsulotomy to treat cataracts.

5. The final set of related mechanisms, grouped under the term photodisruption, are the mechanical effects that can accompany plasma

generation, such as bubble formation, cavitation, jetting and shockwaves. These can be used in lithotripsy (breaking up kidney or gall stones)[18].

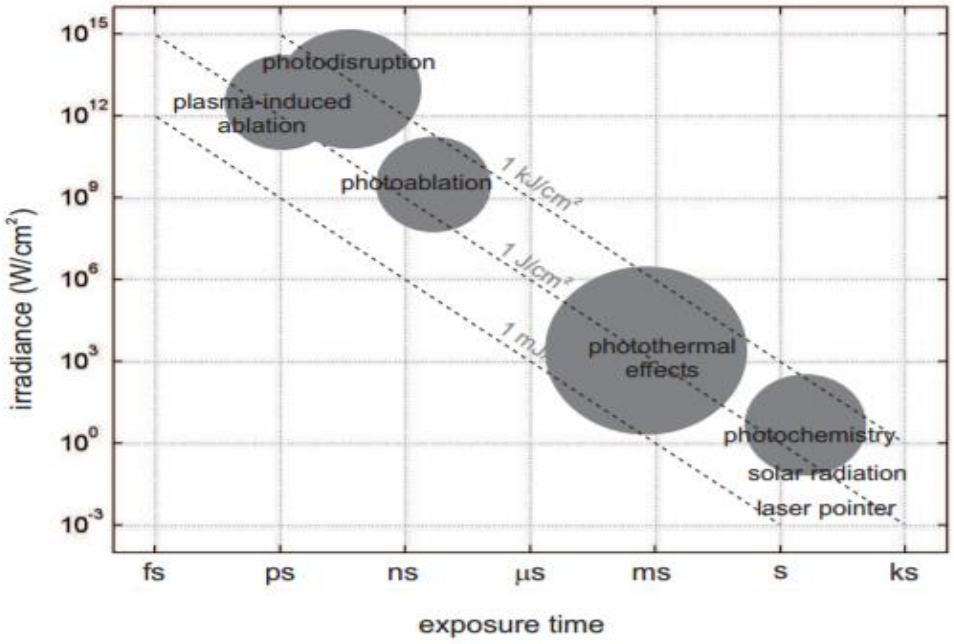

Figure3-6: An overview of the different types of laser-tissue interaction, and the irradiance and exposure durations at which they dominate[18].

3.7.4The equations of interaction between light and blood:

-The simple law of reflection requires the wave normals of the incidentand reflected beams and the normal of the reflecting surface to lie within one plane, called the plane of incidence. It also states that the

reflection angle θ′ equals the angle of incidence θ and expressed by:

$$\theta = \theta' \qquad (3-1)$$

The angles θ and θ′ are measured between the surface normal and the incident and reflected beams, respectively. The surface itself is assumed to be smooth, with surface irregularities being small compared to the wavelength of radiation. This results in so-called specular reflection[19].

-Refraction usually occurs when the reflecting surface separates two media of different indices of refraction. It originates from a change in speed of thelight wave. The simple mathematical relation governing refraction is known as Snell's law. It is given by:

$$\frac{\sin\theta}{\sin\theta''} = \frac{v}{v'} = \qquad (3\text{-}2)$$

where θ′ is the angle of refraction, and v and v′ are the speeds of light in the media before and after the reflecting surface, respectively. Since the corresponding indices of refraction are defined by:

$$n = \frac{c}{v} \qquad (3\text{-}3)$$

$$n' = \frac{c}{v'} \qquad (3\text{-}4)$$

where c denotes the speed of light in vacuum, (3-2) turns into:

$$n \sin\theta = n' \sin\theta'' \qquad (3\text{-}5)$$

Only for sin θ > n′/n can (3-5) not be fulfilled, meaning that refraction will not occur. This event is also referred to as total reflection. The reflectivity of a surface is a measure of the amount of reflected radiation. It is defined as the ratio of reflected and incident electric field amplitudes.

The reflectance is the ratio of the corresponding intensities and is thus equal to the square of the reflectivity. Reflectivity and reflectance depend on the angle of incidence[19].

-During absorption, the intensity of an incident electromagnetic wave is attenuated in passing through a medium. The absorbance of a medium is defined as the ratio of absorbed and incident intensities. Absorption is due to a partial conversion of light energy into heat motion or certain vibrations of molecules

of the absorbing material. A perfectly transparent medium permits the passage of light without any absorption.

Two laws are frequently applied which describe the effect of either thickness or concentration on absorption, respectively. They are commonly called Lambert's law and Beer's law, and are expressed by:

$$I(z) = I0\ exp(-\alpha z) \quad (3\text{-}6)$$

$$I(z) = I0\ exp(-k'\ c\ z) \quad (3\text{-}7)$$

where z denotes the optical axis, $I(z)$ is the intensity at a distance z, $I0$ is the incident intensity, α is the absorption coefficient of the medium, c is the concentration of absorbing agents, and k´ depends on internal parameters other than concentration. Since both laws describe the same behavior of absorption, they are also known as the Lambert–Beer law. From (3-6), we obtain:

$$z = \frac{1}{\alpha} ln\frac{I0}{I(z)} \quad (3\text{-}8)$$

The inverse of the absorption coefficient α is also referred to as the absorption length L

$$L = \frac{1}{\alpha} \quad (3\text{-}9)$$

-When elastically bound charged particles are exposed to electromagnetic waves, the particles are set into motion by the electric field. If the frequency of the wave equals the natural frequency of free vibrations of a particle, resonance occurs being accompanied by a considerable amount of absorption.

Scattering, on the other hand, takes place at frequencies not corresponding to those natural frequencies of particles.

Elastic and inelastic scattering are distinguished, depending on whether part of the incident photon energy is converted during the process of scattering.

A special kind of elastic scattering is Rayleigh scattering. Its only restriction is that the scattering particles be smaller than the wavelength of incident radiation. In particular, we will find a relationship between scattered intensity and index of refraction, and that scattering is inversely proportional to the fourth power of wavelength. The latter statement is also known as Rayleigh's law and shall be derived in the following paragraphs.

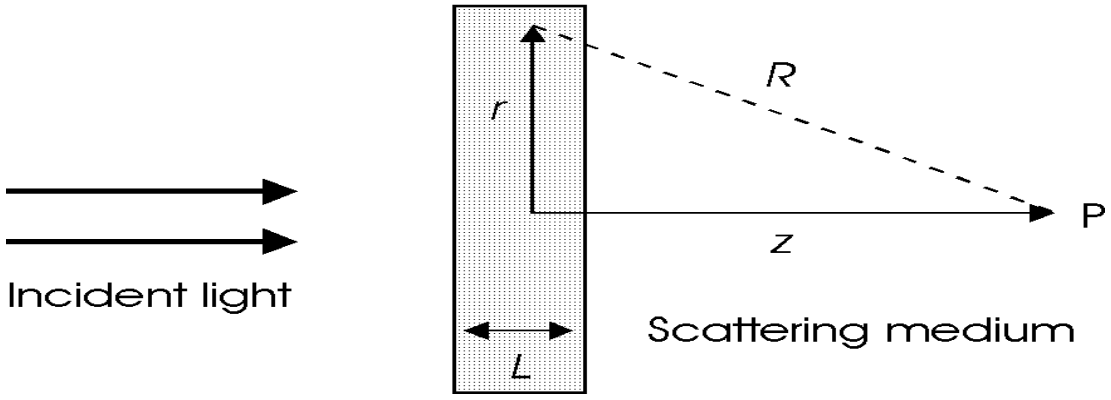

Figure 3-7 : Geometry of Rayleigh scattering[19].

A plane electromagnetic wave is incident on a thin scattering medium with a total thickness L. At a particular time, the electric field of the incident wave can be expressed by:

$$E(z) = E0\ exp(ikz) \qquad (3\text{-}10)$$

where E0 is the amplitude of the incident electric field, k is the amount of the propagation vector, and z denotes the optical axis.

The loss in intensity due to scattering is described by a similar relation as absorption:

$$I(z) = I0\ exp(-\alpha s\ z) \qquad (3\text{-}11)$$

where αs is the scattering coefficient. Differentiation of (3-11) with respect to

z leads to

$$d\,I\; =\; -\,\alpha s\; I\; d\; z \qquad (3\text{-}12)$$

The intensity scattered by a thin medium of a thickness L is thus proportional to αs and L:

$$Is\; \sim \alpha s\; L \qquad (3\text{-}13)$$

3.8 Turbid Media

Total attenuation coefficient can be expressed by:

$$\alpha t = \;\alpha +\; \alpha s \qquad (3\text{-}14)$$

In turbid media, the mean free optical path of incident photons is thus determined by:

$$Lt\; =\; \tfrac{1}{\alpha}\; =\; \tfrac{1}{\alpha+\,\alpha s} \qquad (3\text{-}15)$$

Also, it is very convenient to define an additional parameter, the optical albedo a, by:

$$a\; =\; \tfrac{\alpha s}{\alpha t}\; =\; \tfrac{\alpha s}{\alpha+\,\alpha s} \qquad (3\text{-}16)$$

For a = 0, attenuation is exclusively due to absorption, whereas in the case of a = 1 only scattering occurs.

For a = 1/2, (2.32) can be turned into the equality α = αs, i.e. the coefficients of absorption and scattering are of the same magnitude. In general, both effects will take place but they will occur in variable ratios.

In Fig(3-8), the albedo is shown as a function of the scattering coefficient.

Three different absorption coefficients are assumed which are typical for biological tissue. In addition, the value a = 1/2 is indicated. For αs >> α, the albedo asymptotically approaches unity.

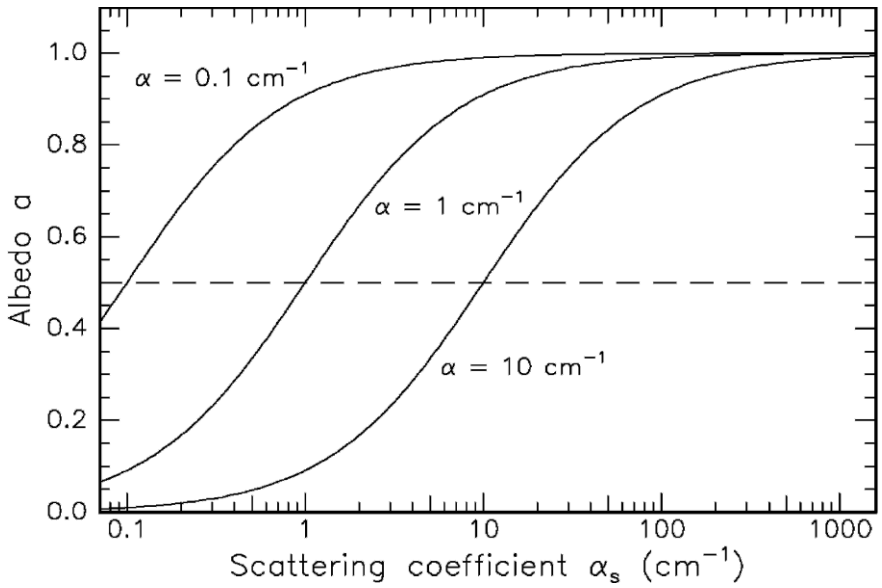

Figure3-8:Optical albedo as a function of scattering coefficient (absorption coefficient :as labeled). The albedo a = 1/2 is indicated[19].

3.9 Photon Transport Theory

A mathematical description of the absorption and scattering characteristics of light can be performed in two different ways: analytical theory or transport theory. The first is based on the physics of Maxwell's equations and is, at least in principle, the most fundamental approach.

However, its applicability is limited due to the complexities involved when deriving exact analytical solutions. Transport theory, on the other hand, directly addresses the transport of photons through absorbing and scattering media without taking Maxwell's equations into account. It is of a heuristic character and lacks the strictness of analytical theories. Nevertheless, transport theory has been used extensively when dealing with laser–tissue interactions, and experimental evidence is given that its predictions are satisfactory in many cases[19].

3.10 Modeling

Models describe our beliefs about how the world functions. In mathematical modeling, we translate those beliefs into the language of mathematics. This has many advantages like , Mathematics is a very precise language; This helps us to formulate ideas and identify underlying assumptions, Mathematics is a concise language; with well-defined rules for manipulations, All the results that mathematicians have proved over hundreds of years are at our disposal and Computers can be used to perform numerical calculations [20].

Mathematical modeling can be used for a number of different reasons. How well any particular objective is achieved depends on both the state of knowledge about a system and how well the modeling is done. Examples of the range of objectives are:

1. Developing scientific understanding

-through quantitative expression of current knowledge of a system (as well as displaying what we know, this may also show up what we do not know).

2. test the effect of changes in a system.

3. aid decision making, including:

(i) tactical decisions by managers.

(ii) strategic decisions by planners.

3.10.1Classifications of models

Models classification according to tow concept:

A) based on the type of outcome they predict:

(i) Deterministic models

ignore random variation, and so always predict the same outcome from a given starting point.

(ii)Stochastic models

May be more statistical in nature and so may predict the distribution of possible outcomes.

B) consider the level of understanding on which the model is based:

(i) Mechanistic models

They take account of the mechanisms through which changes occur.

(ii)Empirical models

No account is taken of the mechanism by which changes to the system occur [20].

3.11 Monte Carlo simulation

Monte Carlo simulation is a type of simulation that relies on repeated random sampling and statistical analysis to compute the results. This method of simulation is very closely related to random experiments, experiments for which the specific result is not known in advance[2].

The Monte Carlo method has been used in various applications, including a very large application code package developed by Los Alamos . In this large-scale Monte Carlo simulation modeling, detailed neutron and photon physics models that contain the up-to-date cross-sections and reaction information were used[20].

Monte Carlo use mathematical models in natural sciences, social sciences, and engineering disciplines to describe the interactions in a system using mathematical expressions . These models typically depend on a number of input parameters,

which when processed through the mathematical formulas in the model, results in one or more outputs. A schematic diagram of the process is shown in Figure(3-9) [2].

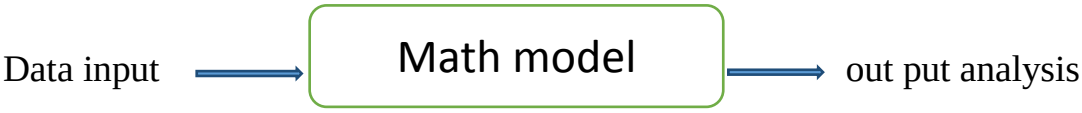

Figure3-9: Mathematical models[2].

The Monte Carlo simulation of light propagation in tissue requires random selection of M photon step size, scattering angle and reflection or transmission at boundaries. This is accomplished by a random number [0,1] assigned to the value of a random variable *x*, such as photon step size[21].

The relationship is established through the density function *p*(*x*) and distribution function *F*(*x*). Given *p*(*x*), the value of the distribution function at a particular value *x*1 of the random variable *x* is

$$F(x1) = \int_0^{x1} P(X)\ dx = function(x1) \qquad (3\text{-}17)$$

This F(x1) is equated with a random number, RND1, in the interval [0,1]:

$$RND1 = F(x1) \qquad (3\text{-}18)$$

The first example is predicting the step size of a photon between interaction events (absorption or scattering) as the photon multiply scatters within a tissue. A photon takes a step(s [cm]) whose length is exponentially distributed, and depends on the value of the total attenuation coefficient equal to μa + μs, where μ*a* is the absorption coefficient and μs is the scattering coefficient.

The value $\frac{1}{\mu t}$ is the photon's mean free pathlength before eitherabsorption or scattering occurs.

The first step is to specify a properly normalized probability density function that describes the probability of a particular step size s[21].

$$p(s) = exp(-\mu ts)/\mu t[15] \quad (3\text{-}19)$$

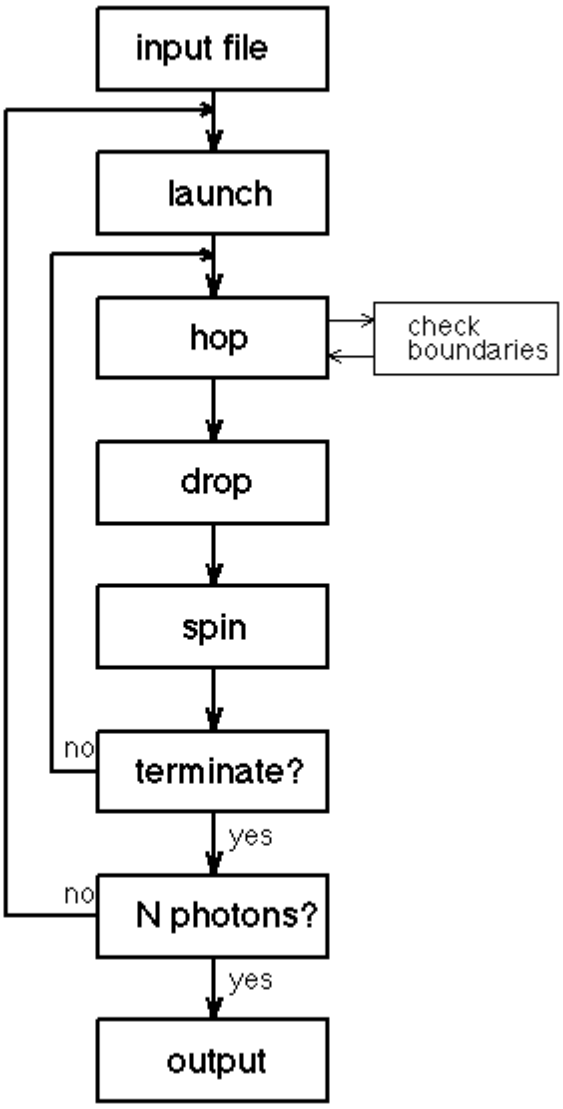

Figure3-10:The flow-diagram for a steady-state Monte Carlo simulation[21].

Chapter Four

Methodology

4.1 Methodology

The methodology focuses on design system to detect malaria parasite depending on basis of mathematical modeling (absorption , scattering co-efficient , refraction and reflection index of human blood). Monte carlo simulation used to measure the probabilities for scattering , absorption , reflection and refraction for normal and abnormal blood according to the parameters and functions.

4.2 The Blood Parameters

According to the wave length were selected (633 nm) determined the:

➢Optical parameters of normal blood

$mua = 0.210 \ \ cm\text{^} - 1$

$mus = 77.3 \ \ cm\text{^} - 1$

$g = 0.994$

$nt = 1.35$

N photons = 10000 (set number of photons in simulation)

Radial _size = 2.0 cm

➢Optical parameters of malaria infected blood

N=1.39

$Mua = 2.304 \ OD \ /e$ (4-1)

E= thickness of sample

OD = optical density

$$OD = \log_{10}(\frac{I0}{I}) \quad (4\text{-}2)$$

I= intensity of light pass through sample

I0= initial light intensity

Suppose the thickness of sample = 2 cm

$OD = 2.07 + 3.09$

$Mua = 2.304 * 5.16 = 5.944\ cm\text{^} - 1$

Laser type is Hi-Ne (infra red spectrum)

Angle of incidence=90 degree

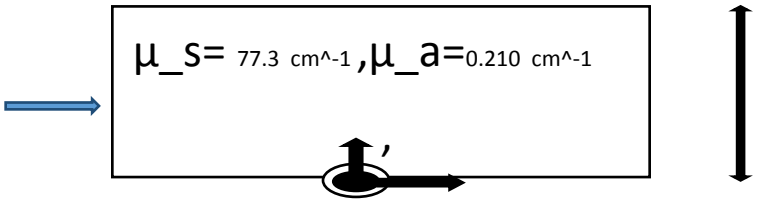

photon beam(laser $\rightarrow \lambda = 633nm, \Theta = 90$ degree)

Figure 4-1: diagram show parameters of light and blood .

The next flowchart(4-2) show the variable step size Monte Carlo technique. The photon packet is initialized. The distance to the first interaction event is found and the photon packet is moved. If the photon has left the tissue, the possibility of internal reflection is checked. If the photon is internally reflected then the photon position is adjusted accordingly and the program continues, otherwise the photon escapes and the event is recorded. For photons which continue, some fraction of the photon packet (1−a)w will be absorbed each step. This fraction is recorded and

the photon weight is adjusted. If the weight is above a minimum, then the rest of the photon packet is scattered into a new direction and the process is repeated. If the weight falls below a minimum, then roulette is played to either extinguish or continue propagating the photon. If the photon does not survive the routette, a new photon packet is started.

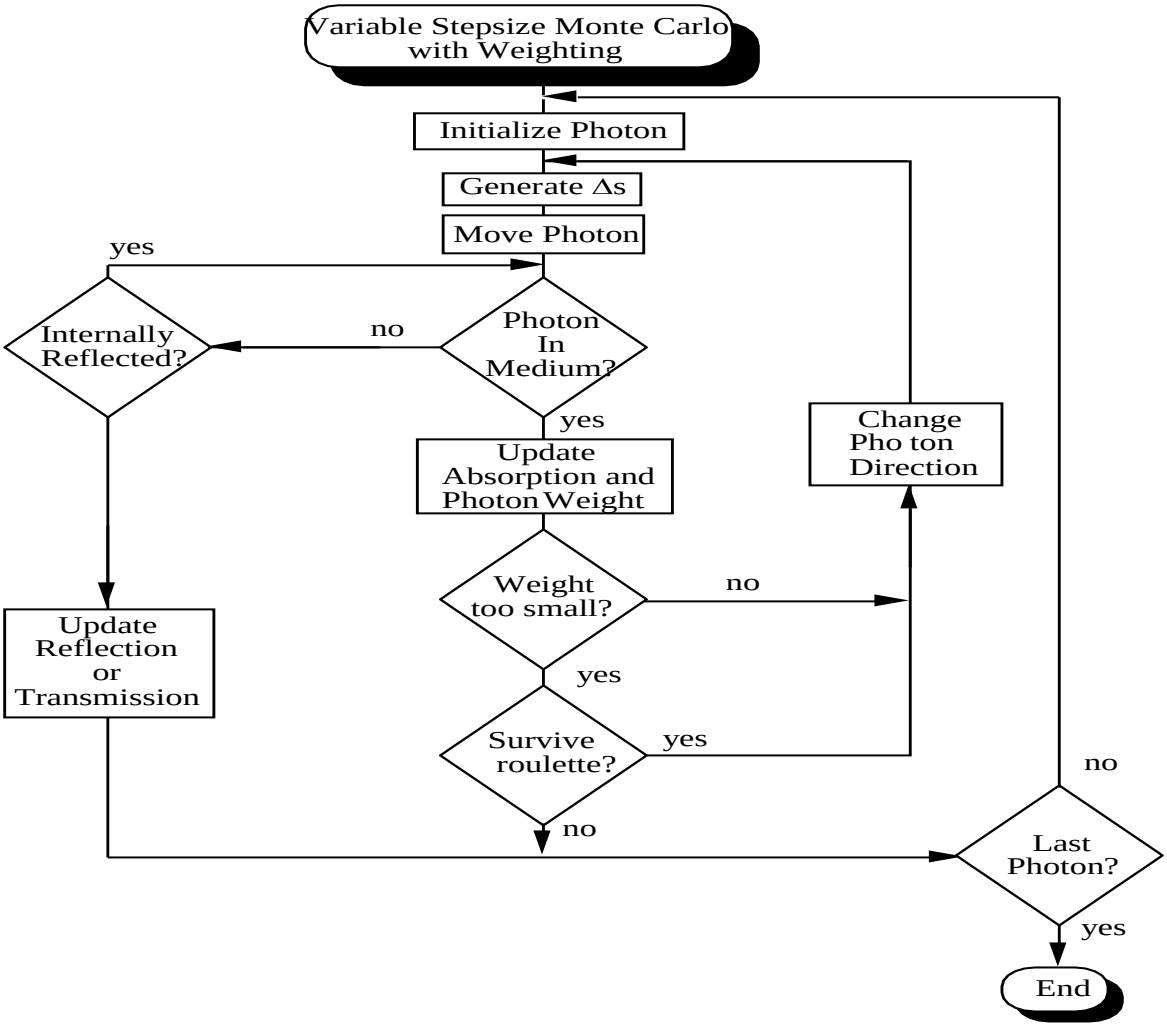

Figure 4-2: Show how Monte Carlo work.

first the parameters for normal blood were entered to Monte Carlo simulation and Monte Carlo calculation the probabilities for each even ,then the parameters for abnormal were entered to Monte Carlo and calculation the probabilities for each

even ,after that compared between probabilities for each blood was done. The next figure show how the parameters for each bloods and functions entered to Monte Carlo .

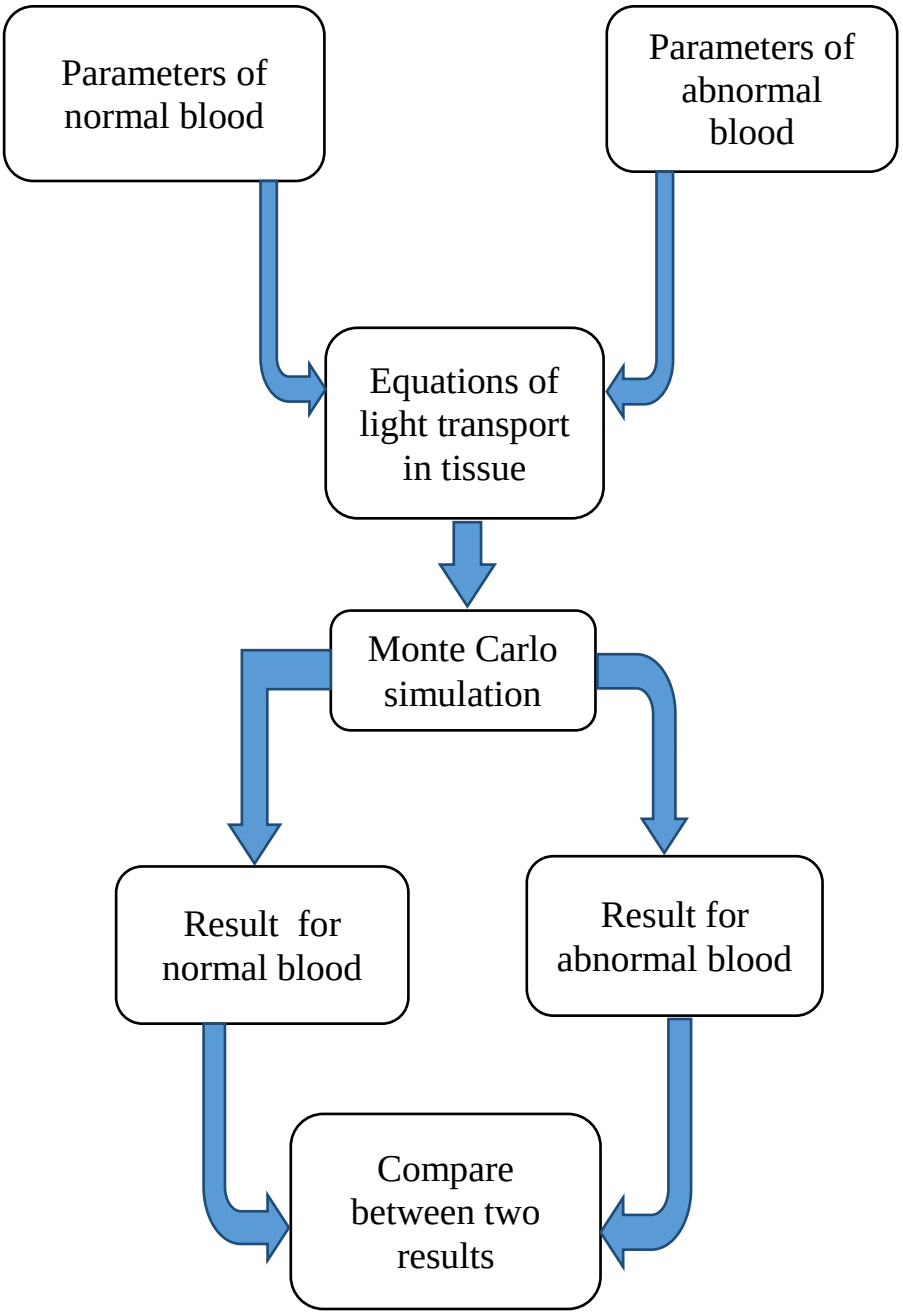

Figure 4-3:show the method used to obtain the data

4.3 Photon propagation

It is based on Jacques steady state Monte Carlo using C standard

Language .

4.3.1 Photon launching

Photon weight was 1 watt and it was launched perpendicular to sample at

x, y, z=0,0,0 .

- generating the propagation distance:

The simplest Monte Carlo method propagates each photon with small, fixed incremental step sizes. The fixed step size Δs must be small relative to the average mean free path length of a photon in the tissue. The mean free path length is the reciprocal of the total attenuation coefficient.

$$\Delta s << 1/\mu t = 1/(\mu s + \mu a) \quad (4\text{-}3)$$

Photon taked step

$$S = -ln(RND1)/\mu t \quad (4\text{-}4)$$

Where S is step function and RND is random value which is Uniformly distributed over interval it range between 0 and 1.

μt is attenuation coefficient .

- Moving the photon

  For a photon located at (x, y ,z) travelling a distance Δs in the direction (μx, μy ,μz), the new coordinates (x0,y0,z0) are given by

  $x0 = x + \mu x\, \Delta s$

$$y0 = y + \mu y\, \Delta s$$
$$z0 = z + \mu z\, \Delta s \qquad (4\text{-}5)$$

4.3.2 Photons reflection

When photons reached boundary they reflected . The reflection was calculated using Fresnel equation

$$R = ((sin\,\theta\, cos\,\theta'' - cos\,\theta\, sin\,\theta'')/(sin\,\theta\, cos\theta'' + cos\theta\, sin\,\theta''))\text{^}2 \qquad (4\text{-}6)$$

Where

R = reflectance

$Sin\ \theta$ = incident angle

$Cos\ \theta$ = incident angle

$Sin\ \theta''$ = reflectance angle

$Cos\ \theta''$ = reflectance angle

The boundary was checked if all photon was reflected then nothing happened . Some photon reflected internally and this calculated by Fresnel Equation

$$R_i = \frac{\sin\theta^2(\sin\theta_1\cos\theta_2 - \cos\theta_1\sin\theta_2)^2}{2} \cdot \frac{\left((\cos\theta_1\cos\theta_2 + \sin\theta_1\sin\theta_2)^2 + (\cos\theta_1\cos\theta_2 - \sin\theta_1\sin\theta_2)^2\right)}{\left((\sin\theta_1\cos\theta_2 + \cos\theta_1\sin\theta_2)^2 (\cos\theta_1\cos\theta_2 + \sin\theta_1\sin\theta_2)^2\right)} \qquad (4\text{-}7)$$

Where

Ri = internal reflection

$Cos\theta 1$=incident trajectory

$sin\theta 1$=incident trajectory

$sin\theta 2$ =transmitted trajectory

$cos\theta 2$ =transmitted trajectory

4.3.3 Absorption

The photons that interacted with blood some of weight Was absorped and other was scattered . The droped weight would be put in bins that defined potions of photon

$$\Delta W = W * (\mu a/\mu t) \quad (4\text{-}8)$$

Where

ΔW = droped weight

W = photon initial weight

μa = absorption coeffiecent

μt = attenuation coefficent

and photon weight was updated

$$W - \Delta W \rightarrow W \quad (4\text{-}9)$$

4.3.4 Scattering event

Photon scattered to new trajecy and this was calculated using

Henyey-Greenstein equation

$$p(\theta) = \frac{1}{4\pi} \frac{1-g^2}{\left(1+g^2-2g\cos\theta\right)^{3/2}} \quad (4\text{-}10)$$

Where

$p(\theta)$ = propability function

g = scattering ancitropy (0.7-0.99)

The Monte Carlo sampling of Henyey-Greenstein equation was

Calculated by

$$\cos(\theta) = \frac{1+g^2 - \left(\frac{1-g^2}{1-g+2g\mathrm{RND}}\right)^2}{2g} \quad (4\text{-}11)$$

Where

RND = random number

After that trajecy would be updated based on value of cos(θ) .

4.3.5 Termination of photon

Photon would be terminated if photon weight if it weight Was not enough here we used routtle method . If Photon weight reached threshold value which is 10^-4

Photon would be terminated as shown below

$$Three\ shold\ =\ (\mu s/\mu t)\text{^}N\ step \quad (4\text{-}12)$$

Where

$N\ step$ = number of step for photon

The time required for running photon was calculated by

$$t = N_{photons}\ t_{per\ .\ step} N_{steps} \quad (4\text{-}13)$$

Where

$N\ photon$ = number of photon

$t\ per\ .step$ = time required per photon step

Chapter Five

Result & Discussions

5.1 Result

This chapter show the results of code implementation using steady state Monte Carlo method for normal blood and malaria blood . It display fluence rate for both normal and abnormal blood .

Those figures(5-1),(5-2),(5-3) below show relation between fluence rate for spherical, cylindrical , planer shells and distance From source for 10000 photons.

And from this figures we get acceptable results from comparing between it and notice that all change happen in shape of shell in tissue (blood) when visible laser light interact With blood in both normal and abnormal which mainly depend on distance from source.

It required only 1 minute for program MESDIV program to display

Statistical data .

Mua of malaria blood was found more than Mua of normal blood .

Mus of malaria blood was found less than Mus of normal blood .

The difference of mua and mus due to change in chemical structure and

so blood consentration will decrease and affects blood density .

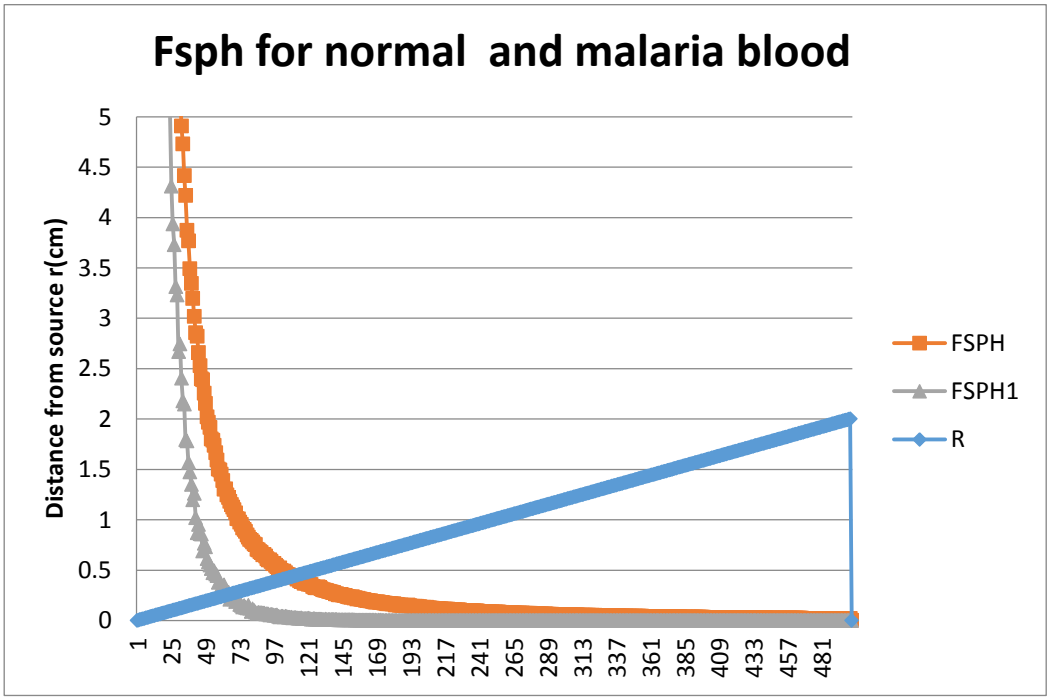

Figure5-1: FSPH for normal and FSPH1 for malaria blood

5000 photon was used with distance 5 cm for spherical shell .

More than 2 cm from source there was no differentiation was noticed but there was high differentiation Under 2cm when photons are less than 199 photons .

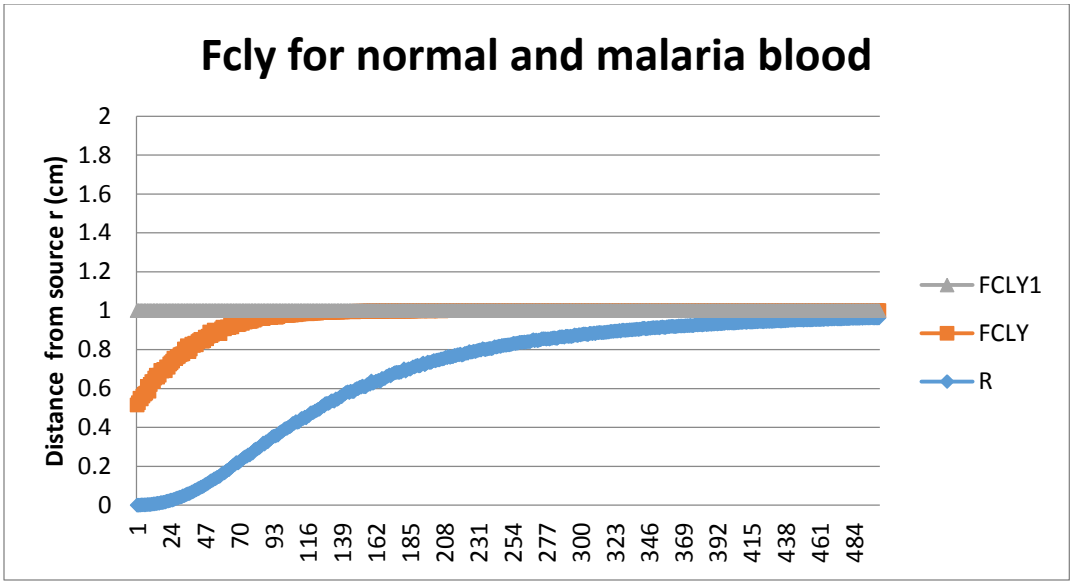

Figure 5-2: FCLY for normal and FCLY1 for malaria blood

5000 photon was used with distance from the source 2 cm for cylindrical shell .

There was differentiation between 0.5 cm and 1cm when photonsare less than 64 photons .

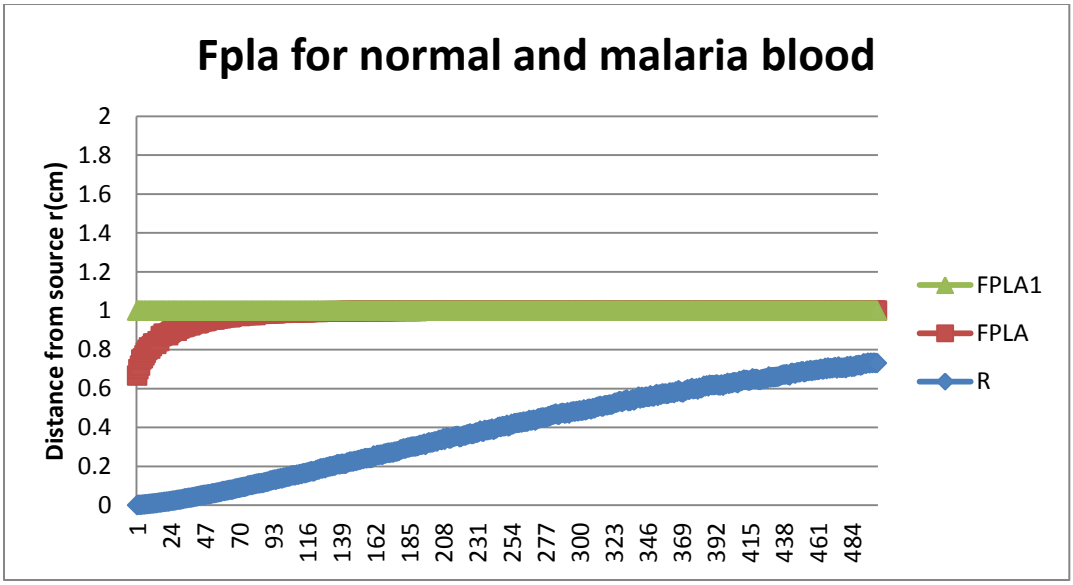

Figure 5-3: FPLA for normal and FPLA1 for malaria blood

5000 photon was used with distance from the source 2cm for planar shell . There was differentiation between 0.6 cm and 1cm when photons are less than 22 photons .

.

Chapter Six

Conclusion and recommendations

6.1 Conclusion

Malaria is big problem especially in Sudan and Africa causing death every year so using current method may be does not provide accurate result and time consuming.

Using Monte Carlo to make modeling it provide way to understand interaction of malaria and light and can help us create device give timely , more accurate and does not depend on human to diagnosis .

6.2 Recommendations

We recommend to

1-Use other wave length to generate model and compare

Result with this model.

2-may be using this method to detect malaria non-invasive by measuring the parameters of skin layers.

3-Make device based on model.

4- Enter the data obtained from model to classifier to give more accurate result for detect malaria.

Reference

[1] FEG Cox - Parasites & vectors, 2010 – parasites and vectors. Bio med central.

[2] An Introduction to Mathematical Modeling Glenn Marion, Bioinformatics and Statistics Scotland Given 2008 by Daniel Lawson and Glenn Marion.

[3] Jurovata, Dominika, et al. "Simulation of Photon Propagation in Tissue Using Matlab." Vedecké Práce Materiálovotechnologickej Fakulty Slovenskej.

[4] Prahl, Scott A., et al. "A Monte Carlo model of light propagation in tissue." Dosimetry of laser radiation in medicine and biology 5 (1989): 102-111.

[5] Shirkavand, Afshan, et al. "A new Monte Carlo code for absorption simulation of laser-skin tissue interaction." Chinese Optics Letters 5.4 (2007): 238-240.

[6] https://patient.info/in/health/blood.

[7] http://www.medicinenet.com/hemoglobin/article.htm.

[8] https://**www.cdc.gov**/**malaria**/about/**biology**.

[9] **www.who.int**/mediacentre/factsheets/fs094.

[10] https://www.cdc.gov/malaria/malaria_worldwide/impact.html.

[11] Dave M. Newman, John Heptinstall,…etc ,(2008),A Magneto-Optic Route toward the In Vivo Diagnosis of Malaria :Preliminary Results and Preclinical Trial Data, University of Exeter, Exeter EX4 4QF, United Kingdom; Biophysical Journal Volume 95 July 2008 -3495/08/07/994/07.

[12] T. Nishita, Y. Miyawaki, and E. Nakamae ,” A shading model for atmospheric scattering considering luminous intensity distribution of light

sources", In Proceedings of SIGGRAPH'87, pages 303–310. ACM Press, July 1987.

[13] Mohandas, Narla, and Xiuli An."Malaria and human red blood cells."Medical Microbiology and immunology 201.4 (2012): 593-598.

[14] http://m.onlymyhealth.com/amp/how-does-malaria-affect-the-red-blood-cells-1384781167.

[15] Singh, Gurjeet, et al. "Effects of malarial parasitic infections on human blood cells." *Int. J. Curr. Microbiol. App. Sci* 3.12 (2014): 622-632.

[16] Yim, D., et al. *On the modeling of light interactions with human blood*. Technical Report CS-2011-30, School of Computer Science, University of Waterloo, 2011.

[17] Muer J,Peltomäki M ,Pobletes ,Gompper G, Fedosov DA(2017) Static and dynamic light scattering by red blood cell: A numerical study.

[18] B Cox - PHAS, 2007 - academia.edu.

[19] Niemz, Markolf H. *Laser-tissue interactions: fundamentals and applications*. Springer Science & Business Media, 2007.

[20] Qin, Jun. "Computational analysis and Monte Carlo simulation of wave propagation." *International Journal of Computational Biology and Drug Design* 8.2 (2015): 159-167

[21] In *Optical-Thermal Responses of Laser-Irradiated Tissue*, 2nd Edition, 2009 eds. A.J. Welch, M.J.C. van Gemert, publ. Springer.

[22] Lee, Seungjun, and Wei Lu. "Backward elastic light scattering of malaria infected red blood cells." Applied Physics Letters 99.7 (2011): 073704.

Appendix

➢The code which used to generation photons (for normal blood)

```
#include <math.h>
#include <stdio.h>
#define Nbins 500
#define Nbinsp1 501
#define PI 3.1415926
#define LIGHTSPEED 2.997925E10 /* in vacuo speed of light [cm/s] */
#define ALIVE 1 /* if photon not yet terminated */
#define DEAD 0 /* if photon is to be terminated */
#define THRESHOLD 0.01 /* used in roulette */
#define CHANCE 0.1 /* used in roulette */
#define COS90D 1.0E-6
/* If cos(theta) <= COS90D, theta >= PI/2 - 1e-6 rad. */
#define ONE_MINUS_COSZERO 1.0E-12
/* If 1-cos(theta) <= ONE_MINUS_COSZERO, fabs(theta) <= 1e-6 rad. */
/* If 1+cos(theta) <= ONE_MINUS_COSZERO, fabs(PI-theta) <= 1e-6 rad. */
#define SIGN(x) ((x)>=0 ? 1:-1)
#define InitRandomGen (double) RandomGen(0, 1, NULL)
/* Initializes the seed for the random number generator. */
#define RandomNum (double) RandomGen(1, 0, NULL)
/* Calls for a random number from the randum number generator. */
/* DECLARE FUNCTION */
double RandomGen(char Type, long Seed, long *Status);
```

```
/* Random number generator */
main() {
/* Propagation parameters */
double x, y, z; /* photon position */
double ux, uy, uz; /* photon trajectory as cosines */
double uxx, uyy, uzz; /* temporary values used during SPIN */
double s; /* step sizes. s = -log(RND)/mus [cm] */
double costheta; /* cos(theta) */
double sintheta; /* sin(theta) */
double cospsi; /* cos(psi) */
double sinpsi; /* sin(psi) */
double psi; /* azimuthal angle */
double i_photon; /* current photon */

double W; /* photon weight */
double absorb; /* weighted deposited in a step due to absorption */
short photon_status; /* flag = ALIVE=1 or DEAD=0 */
/* other variables */
double Csph[Nbinsp1]; /* spherical photon concentration CC[ir=0..100] */
double Ccyl[Nbinsp1]; /* cylindrical photon concentration CC[ir=0..100] */
double Cpla[Nbinsp1]; /* planar photon concentration CC[ir=0..100] */
double Fsph; /* fluence in spherical shell */
double Fcyl; /* fluence in cylindrical shell */
double Fpla; /* fluence in planar shell */
double mua; /* absorption coefficient [cm^-1] */
double mus; /* scattering coefficient [cm^-1] */
double g; /* anisotropy [-] */
```

```
double albedo; /* albedo of tissue */
double nt; /* tissue index of refraction */
double Nphotons; /* number of photons in simulation */
short NR; /* number of radial positions */
double radial_size; /* maximum radial size */
double r; /* radial position */
double dr; /* radial bin size */
short ir; /* index to radial position */
double shellvolume; /* volume of shell at radial position r */
double CNT; /* total count of photon weight summed over all bins */
/* dummy variables */
double rnd; /* assigned random value 0-1 */
short i, j; /* dummy indices */
double u, temp; /* dummy variables */
FILE* target; /* point to output file */
/**** INPUT
Input the optical properties
Input the bin and array sizes
Input the number of photons
*****/
mua = 0.210 /* cm^-1
mus = 77.3 /* cm^-1
g = 0.994
nt = 1.35
Nphotons = 10000; /* set number of photons in simulation */
radial_size = 2.0; /* cm, total range over which bins extend */
```

```
NR = Nbins; /* set number of bins. */
/* IF NR IS ALTERED, THEN USER MUST ALSO ALTER THE ARRAY DECLARATION TO A SIZE =
NR+1. */
dr = radial_size/NR; /* cm */
albedo = mus/(mus + mua);
/**** INITIALIZATIONS
*****/
i_photon = 0;
InitRandomGen;
for (ir=0; ir<=NR; ir++) {
Csph[ir] = 0;
Ccyl[ir] = 0;
Cpla[ir] = 0;
}

/**** RUN
Launch N photons, initializing each one before progation.
*****/
do {
/**** LAUNCH
Initialize photon position and trajectory.
Implements an isotropic point source.
*****/
i_photon += 1; /* increment photon count */
if ( fmod(i_photon, Nphotons/10) == 0)
printf("%0.0f%% done\n", i_photon/Nphotons*100);
```

```
W = 1.0; /* set photon weight to one */
photon_status = ALIVE; /* Launch an ALIVE photon */
x = 0; /* Set photon position to origin. */
y = 0;
z = 0;
/* Randomly set photon trajectory to yield an isotropic source. */
costheta = 2.0*RandomNum - 1.0;
sintheta = sqrt(1.0 - costheta*costheta); /* sintheta is always positive */
psi = 2.0*PI*RandomNum;
ux = sintheta*cos(psi);
uy = sintheta*sin(psi);
uz = costheta;
/* HOP_DROP_SPIN_CHECK
Propagate one photon until it dies as determined by ROULETTE.
*******/
do {
/**** HOP
Take step to new position
s = step size
ux, uy, uz are cosines of current photon trajectory
*****/
while ((rnd = RandomNum) <= 0.0); /* yields 0 < rnd <= 1 */
s = -log(rnd)/(mua + mus); /* Step size. Note: log() is base e */
x += s * ux; /* Update positions. */
y += s * uy;
z += s * uz;
/**** DROP
```

```
Drop photon weight (W) into local bin.
*****/
absorb = W*(1 - albedo); /* photon weight absorbed at this step */
W -= absorb; /* decrement WEIGHT by amount absorbed */
/* spherical */
r = sqrt(x*x + y*y + z*z); /* current spherical radial position */
ir = (short)(r/dr); /* ir = index to spatial bin */
if (ir >= NR) ir = NR; /* last bin is for overflow */
Csph[ir] += absorb; /* DROP absorbed weight into bin */

/* cylindrical */
r = sqrt(x*x + y*y); /* current cylindrical radial position */
ir = (short)(r/dr); /* ir = index to spatial bin */
if (ir >= NR) ir = NR; /* last bin is for overflow */
Ccyl[ir] += absorb; /* DROP absorbed weight into bin */
/* planar */
r = fabs(z); /* current planar radial position */
ir = (short)(r/dr); /* ir = index to spatial bin */
if (ir >= NR) ir = NR; /* last bin is for overflow */
Cpla[ir] += absorb; /* DROP absorbed weight into bin */
/**** SPIN
Scatter photon into new trajectory defined by theta and psi.
Theta is specified by cos(theta), which is determined
based on the Henyey-Greenstein scattering function.
Convert theta and psi into cosines ux, uy, uz.
*****/
/* Sample for costheta */
```

```
rnd = RandomNum;
if (g == 0.0)
costheta = 2.0*rnd - 1.0;
else {
double temp = (1.0 - g*g)/(1.0 - g + 2*g*rnd);
costheta = (1.0 + g*g - temp*temp)/(2.0*g);
}
sintheta = sqrt(1.0 - costheta*costheta); /* sqrt() is faster than sin(). */
/* Sample psi. */
psi = 2.0*PI*RandomNum;
cospsi = cos(psi);
if (psi < PI)
sinpsi = sqrt(1.0 - cospsi*cospsi); /* sqrt() is faster than sin(). */
else
sinpsi = -sqrt(1.0 - cospsi*cospsi);
/* New trajectory. */
if (1 - fabs(uz) <= ONE_MINUS_COSZERO) { /* close to perpendicular. */
uxx = sintheta * cospsi;
uyy = sintheta * sinpsi;
uzz = costheta * SIGN(uz); /* SIGN() is faster than division. */
}
else { /* usually use this option */
temp = sqrt(1.0 - uz * uz);
uxx = sintheta * (ux * uz * cospsi - uy * sinpsi) / temp + ux * costheta;
uyy = sintheta * (uy * uz * cospsi + ux * sinpsi) / temp + uy * costheta;
uzz = -sintheta * cospsi * temp + uz * costheta;
}
```

```
/* Update trajectory */
ux = uxx;
uy = uyy;
uz = uzz;
/**** CHECK ROULETTE
If photon weight below THRESHOLD, then terminate photon using Roulette technique.
Photon has CHANCE probability of having its weight increased by factor of 1/CHANCE,
and 1-CHANCE probability of terminating.
*****/
if (W < THRESHOLD) {
if (RandomNum <= CHANCE)
W /= CHANCE;
else photon_status = DEAD;
}
} /* end STEP_CHECK_HOP_SPIN */
while (photon_status == ALIVE);
/* If photon dead, then launch new photon. */
} /* end RUN */
while (i_photon < Nphotons);
/**** SAVE
Convert data to relative fluence rate [cm^-2] and save to file called "mcmin321.out".
*****/
target = fopen("mc321.out", "w");
```

```
/* print header */
fprintf(target, "number of photons = %f\n", Nphotons);
fprintf(target, "bin size = %5.5f [cm] \n", dr);
fprintf(target, "last row is overflow. Ignore.\n");

/* print column titles */
fprintf(target, "r [cm] \t Fsph [1/cm2] \t Fcyl [1/cm2] \t Fpla [1/cm2]\n");
/* print data: radial position, fluence rates for 3D, 2D, 1D geometries */
for (ir=0; ir<=NR; ir++) {
/* r = sqrt(1.0/3 - (ir+1) + (ir+1)*(ir+1))*dr; */
r = (ir + 0.5)*dr;
shellvolume = 4.0*PI*r*r*dr; /* per spherical shell */
Fsph = Csph[ir]/Nphotons/shellvolume/mua;
shellvolume = 2.0*PI*r*dr; /* per cm length of cylinder */
Fcyl = Ccyl[ir]/Nphotons/shellvolume/mua;
shellvolume = dr; /* per cm2 area of plane */
Fpla =Cpla[ir]/Nphotons/shellvolume/mua;
fprintf(target, "%5.5f \t %4.3e \t %4.3e \t %4.3e \n", r, Fsph, Fcyl, Fpla);
}
fclose(target);
} /* end of main */


#define MBIG 1000000000
#define MSEED 161803398
#define MZ 0
#define FAC 1.0E-9
```

```
double RandomGen(char Type, long Seed, long *Status){
static long i1, i2, ma[56]; /* ma[0] is not used. */
long mj, mk;
short i, ii;
if (Type == 0) { /* set seed. */
mj = MSEED - (Seed < 0 ? -Seed : Seed);
mj %= MBIG;
ma[55] = mj;
mk = 1;
for (i = 1; i <= 54; i++) {
ii = (21 * i) % 55;
ma[ii] = mk;
mk = mj - mk;
if (mk < MZ)
mk += MBIG;
mj = ma[ii];
}
for (ii = 1; ii <= 4; ii++)
for (i = 1; i <= 55; i++) {
ma[i] -= ma[1 + (i + 30) % 55];
if (ma[i] < MZ)
ma[i] += MBIG;
}
i1 = 0;
i2 = 31;
} else if (Type == 1) { /* get a number. */
if (++i1 == 56)
```

```
i1 = 1;
if (++i2 == 56)
i2 = 1;
mj = ma[i1] - ma[i2];
if (mj < MZ)
mj += MBIG;
ma[i1] = mj;
return (mj * FAC);
} else if (Type == 2) { /* get status. */
for (i = 0; i < 55; i++)
Status[i] = ma[i + 1];
Status[55] = i1;
Status[56] = i2;
} else if (Type == 3) { /* restore status. */

for (i = 0; i < 55; i++)
ma[i + 1] = Status[i];
i1 = Status[55];
i2 = Status[56];
} else
puts("Wrong parameter to RandomGen().");
return (0);
}

#undef MBIG
#undef MSEED
#undef MZ
```

#undef FAC

- The output from monte carlo simulation (normal blood)

number of photons = 10000.000000

bin size = 0.00400 [cm]

last row is overflow. Ignore.

r [cm]	Fsph [1/cm2]	Fcyl [1/cm2]	Fpla [1/cm2]
0.00200	2.014e+004	1.225e+002	8.157e+000
0.00600	2.202e+003	4.217e+001	6.497e+000
0.01000	7.848e+002	2.473e+001	6.057e+000
0.01400	4.213e+002	1.808e+001	5.922e+000
0.01800	2.436e+002	1.342e+001	5.534e+000
0.02200	1.623e+002	1.114e+001	5.488e+000
0.02600	1.158e+002	9.715e+000	5.251e+000
0.03000	8.923e+001	8.526e+000	5.072e+000
0.03400	6.830e+001	7.497e+000	4.935e+000
0.03800	5.545e+001	6.626e+000	4.764e+000
0.04200	4.482e+001	5.907e+000	4.709e+000
0.04600	3.855e+001	5.437e+000	4.596e+000
0.05000	3.178e+001	4.997e+000	4.530e+000
0.05400	2.746e+001	4.755e+000	4.443e+000
0.05800	2.442e+001	4.240e+000	4.337e+000
0.06200	2.093e+001	4.033e+000	4.342e+000
0.06600	1.843e+001	3.715e+000	4.298e+000
0.07000	1.647e+001	3.594e+000	4.244e+000
0.07400	1.508e+001	3.397e+000	4.088e+000
0.07800	1.303e+001	3.161e+000	4.039e+000
0.08200	1.222e+001	3.074e+000	3.939e+000
0.08600	1.081e+001	2.914e+000	4.064e+000

0.09000	9.891e+000	2.840e+000	3.937e+000
0.09400	9.007e+000	2.614e+000	3.891e+000
0.09800	8.370e+000	2.629e+000	3.891e+000
0.10200	7.889e+000	2.476e+000	3.847e+000
0.10600	7.112e+000	2.356e+000	3.891e+000
0.11000	6.621e+000	2.267e+000	3.694e+000
0.11400	6.177e+000	2.207e+000	3.727e+000
0.11800	5.750e+000	2.109e+000	3.674e+000
0.12200	5.524e+000	2.078e+000	3.657e+000
0.12600	4.909e+000	1.966e+000	3.530e+000
0.13000	4.731e+000	1.985e+000	3.441e+000
0.13400	4.415e+000	1.861e+000	3.542e+000
0.13800	4.218e+000	1.828e+000	3.510e+000
0.14200	3.872e+000	1.766e+000	3.419e+000
0.14600	3.768e+000	1.726e+000	3.397e+000
0.15000	3.493e+000	1.710e+000	3.366e+000
0.15400	3.345e+000	1.658e+000	3.409e+000
0.15800	3.197e+000	1.592e+000	3.368e+000
0.16200	3.019e+000	1.542e+000	3.336e+000
0.16600	2.857e+000	1.490e+000	3.267e+000
0.17000	2.821e+000	1.482e+000	3.218e+000
0.17400	2.661e+000	1.438e+000	3.200e+000
0.17800	2.529e+000	1.397e+000	3.150e+000
0.18200	2.398e+000	1.385e+000	3.158e+000
0.18600	2.390e+000	1.345e+000	3.156e+000
0.19000	2.255e+000	1.303e+000	3.137e+000
0.19400	2.155e+000	1.304e+000	3.095e+000
0.19800	2.020e+000	1.275e+000	3.179e+000
0.20200	1.968e+000	1.209e+000	3.140e+000
0.20600	1.916e+000	1.214e+000	3.062e+000
0.21000	1.802e+000	1.198e+000	3.123e+000

0.21400	1.789e+000	1.183e+000	3.085e+000
0.21800	1.740e+000	1.139e+000	3.090e+000
0.22200	1.667e+000	1.131e+000	3.069e+000
0.22600	1.592e+000	1.110e+000	3.025e+000
0.23000	1.504e+000	1.079e+000	2.986e+000
0.23400	1.495e+000	1.074e+000	2.938e+000
0.23800	1.452e+000	1.058e+000	2.937e+000
0.24200	1.389e+000	1.033e+000	2.948e+000
0.24600	1.305e+000	1.015e+000	2.936e+000
0.25000	1.307e+000	1.003e+000	2.879e+000
0.25400	1.246e+000	9.743e-001	2.885e+000
0.25800	1.222e+000	9.401e-001	2.914e+001
0.26200	1.183e+000	9.252e-001	2.915e+000
0.26600	1.152e+000	9.147e-001	2.864e+000
0.27000	1.125e+000	8.835e-001	2.847e+000
0.27400	1.101e+000	8.994e-001	2.812e+000
0.27800	1.068e+000	8.908e-001	2.796e+000
0.28200	1.010e+000	8.738e-001	2.779e+000
0.28600	1.008e+000	8.434e-001	2.771e+000
0.29000	9.768e-001	8.414e-001	2.764e+000
0.29400	9.541e-001	8.189e-001	2.782e+000
0.29800	9.200e-001	8.249e-001	2.725e+000
0.30200	9.028e-001	8.149e-001	2.667e+000
0.30600	8.856e-001	8.139e-001	2.663e+000
0.31000	8.491e-001	7.815e-001	2.649e+000
0.31400	8.261e-001	8.049e-001	2.660e+000
0.31800	8.039e-001	7.517e-001	2.610e+000
0.32200	7.964e-001	7.488e-001	2.602e+000
0.32600	7.794e-001	7.527e-001	2.582e+000
0.33000	7.593e-001	7.486e-001	2.590e+000
0.33400	7.553e-001	7.376e-001	2.595e+000

0.33800	7.078e-001	7.230e-001	2.587e+000
0.34200	7.009e-001	6.868e-001	2.621e+000
0.34600	6.854e-001	7.181e-001	2.600e+000
0.35000	6.756e-001	6.875e-001	2.598e+000
0.35400	6.512e-001	6.942e-001	2.549e+000
0.35800	6.553e-001	6.690e-001	2.546e+000
0.36200	6.411e-001	6.627e-001	2.483e+000
0.36600	6.132e-001	6.522e-001	2.514e+000
0.37000	6.009e-001	6.484e-001	2.441e+000
0.37400	6.013e-001	6.498e-001	2.457e+000
0.37800	5.860e-001	6.416e-001	2.496e+000
0.38200	5.623e-001	6.471e-001	2.446e+000
0.38600	5.672e-001	6.304e-001	2.462e+000
0.39000	5.469e-001	6.220e-001	2.416e+000
0.39400	5.339e-001	6.199e-001	2.454e+000
0.39800	5.162e-001	6.093e-001	2.402e+000
0.40200	5.215e-001	6.005e-001	2.442e+000
0.40600	4.969e-001	5.959e-001	2.391e+000
0.41000	4.882e-001	5.892e-001	2.382e+000
0.41400	4.905e-001	5.950e-001	2.395e+000
0.41800	4.741e-001	5.795e-001	2.331e+000
0.42200	4.580e-001	5.646e-001	2.321e+000
0.42600	4.557e-001	5.717e-001	2.349e+000
0.43000	4.339e-001	5.507e-001	2.351e+000
0.43400	4.457e-001	5.662e-001	2.324e+000
0.43800	4.363e-001	5.681e-001	2.351e+000
0.44200	4.350e-001	5.501e-001	2.329e+000
0.44600	4.307e-001	5.386e-001	2.329e+000
0.45000	4.118e-001	5.443e-001	2.304e+000
0.45400	4.133e-001	5.360e-001	2.297e+000
0.45800	3.937e-001	5.464e-001	2.301e+000

0.46200	3.862e-001	5.292e-001	2.284e+000
0.46600	3.865e-001	5.352e-001	2.278e+000
0.47000	3.687e-001	5.070e-001	2.231e+000
0.47400	3.740e-001	5.117e-001	2.242e+000
0.47800	3.709e-001	5.113e-001	2.278e+000
0.48200	3.604e-001	5.036e-001	2.271e+000
0.48600	3.599e-001	4.988e-001	2.226e+000
0.49000	3.556e-001	4.979e-001	2.183e+000
0.49400	3.373e-001	4.958e-001	2.194e+000
0.49800	3.319e-001	4.840e-001	2.135e+000
0.50200	3.245e-001	4.757e-001	2.163e+000
0.50600	3.255e-001	4.796e-001	2.133e+000
0.51000	3.341e-001	4.583e-001	2.176e+000
0.51400	3.301e-001	4.597e-001	2.134e+000
0.51800	3.168e-001	4.654e-001	2.121e+000
0.52200	3.063e-001	4.593e-001	2.097e+000
0.52600	3.019e-001	4.494e-001	2.103e+000
0.53000	2.989e-001	4.519e-001	2.095e+000
0.53400	2.967e-001	4.581e-001	2.101e+000
0.53800	2.897e-001	4.413e-001	2.087e+000
0.54200	2.866e-001	4.463e-001	2.053e+000
0.54600	2.833e-001	4.403e-001	2.038e+000
0.55000	2.788e-001	4.313e-001	2.071e+000
0.55400	2.770e-001	4.329e-001	2.043e+000
0.55800	2.640e-001	4.205e-001	2.073e+000
0.56200	2.665e-001	4.145e-001	2.080e+000
0.56600	2.561e-001	4.080e-001	2.095e+000
0.57000	2.569e-001	4.030e-001	2.031e+000
0.57400	2.594e-001	4.127e-001	2.039e+000
0.57800	2.526e-001	4.032e-001	2.006e+000
0.58200	2.504e-001	4.108e-001	2.020e+000

0.58600	2.482e-001	4.099e-001	2.032e+000
0.59000	2.411e-001	4.001e-001	2.014e+000
0.59400	2.379e-001	3.947e-001	2.026e+000
0.59800	2.331e-001	3.991e-001	1.993e+000
0.60200	2.287e-001	3.892e-001	2.003e+000
0.60600	2.353e-001	3.889e-001	1.987e+000
0.61000	2.223e-001	3.833e-001	1.962e+000
0.61400	2.273e-001	3.931e-001	1.975e+000
0.61800	2.149e-001	3.945e-001	1.945e+000
0.62200	2.215e-001	3.816e-001	1.969e+000
0.62600	2.144e-001	3.776e-001	1.971e+000
0.63000	2.125e-001	3.807e-001	1.983e+000
0.63400	2.070e-001	3.583e-001	1.979e+000
0.63800	2.066e-001	3.787e-001	1.979e+000
0.64200	2.024e-001	3.708e-001	1.884e+000
0.64600	1.995e-001	3.650e-001	1.922e+000
0.65000	1.971e-001	3.650e-001	1.885e+000
0.65400	1.944e-001	3.630e-001	1.885e+000
0.65800	1.945e-001	3.734e-001	1.888e+000
0.66200	1.886e-001	3.514e-001	1.886e+000
0.66600	1.848e-001	3.576e-001	1.914e+000
0.67000	1.827e-001	3.559e-001	1.852e+000
0.67400	1.845e-001	3.435e-001	1.876e+000
0.67800	1.868e-001	3.435e-001	1.853e+000
0.68200	1.798e-001	3.352e-001	1.840e+000
0.68600	1.779e-001	3.441e-001	1.877e+000
0.69000	1.779e-001	3.335e-001	1.858e+000
0.69400	1.736e-001	3.290e-001	1.877e+000
0.69800	1.728e-001	3.255e-001	1.847e+000
0.70200	1.655e-001	3.242e-001	1.860e+000
0.70600	1.650e-001	3.271e-001	1.850e+000

0.71000	1.664e-001	3.298e-001	1.845e+000
0.71400	1.676e-001	3.278e-001	1.788e+000
0.71800	1.629e-001	3.201e-001	1.788e+000
0.72200	1.659e-001	3.079e-001	1.756e+000
0.72600	1.537e-001	3.270e-001	1.777e+000
0.73000	1.595e-001	3.190e-001	1.768e+000
0.73400	1.557e-001	3.120e-001	1.745e+000
0.73800	1.518e-001	3.157e-001	1.762e+000
0.74200	1.527e-001	3.097e-001	1.739e+000
0.74600	1.501e-001	3.043e-001	1.736e+000
0.75000	1.521e-001	3.047e-001	1.738e+000
0.75400	1.471e-001	2.986e-001	1.746e+000
0.75800	1.435e-001	2.964e-001	1.750e+000
0.76200	1.526e-001	3.021e-001	1.742e+000
0.76600	1.464e-001	3.018e-001	1.712e+000
0.77000	1.406e-001	2.913e-001	1.716e+000
0.77400	1.417e-001	2.846e-001	1.715e+000
0.77800	1.390e-001	2.982e-001	1.690e+000
0.78200	1.424e-001	2.916e-001	1.746e+000
0.78600	1.413e-001	2.835e-001	1.698e+000
0.79000	1.357e-001	2.860e-001	1.658e+000
0.79400	1.377e-001	2.873e-001	1.682e+000
0.79800	1.327e-001	2.813e-001	1.685e+000
0.80200	1.290e-001	2.764e-001	1.692e+000
0.80600	1.324e-001	2.791e-001	1.659e+000
0.81000	1.273e-001	2.771e-001	1.661e+000
0.81400	1.328e-001	2.768e-001	1.670e+000
0.81800	1.256e-001	2.758e-001	1.622e+000
0.82200	1.264e-001	2.706e-001	1.624e+000
0.82600	1.222e-001	2.729e-001	1.646e+000
0.83000	1.219e-001	2.713e-001	1.589e+000

0.83400	1.162e-001	2.640e-001	1.648e+000
0.83800	1.174e-001	2.668e-001	1.581e+000
0.84200	1.181e-001	2.594e-001	1.589e+000
0.84600	1.182e-001	2.669e-001	1.631e+000
0.85000	1.157e-001	2.647e-001	1.641e+000
0.85400	1.148e-001	2.661e-001	1.597e+000
0.85800	1.122e-001	2.568e-001	1.594e+000
0.86200	1.122e-001	2.597e-001	1.574e+000
0.86600	1.134e-001	2.544e-001	1.578e+000
0.87000	1.120e-001	2.547e-001	1.584e+000
0.87400	1.121e-001	2.517e-001	1.639e+000
0.87800	1.090e-001	2.598e-001	1.633e+000
0.88200	1.080e-001	2.554e-001	1.604e+000
0.88600	1.051e-001	2.498e-001	1.592e+000
0.89000	1.049e-001	2.499e-001	1.601e+000
0.89400	1.068e-001	2.504e-001	1.566e+000
0.89800	1.045e-001	2.401e-001	1.569e+000
0.90200	1.054e-001	2.463e-001	1.550e+000
0.90600	1.047e-001	2.446e-001	1.580e+000
0.91000	1.010e-001	2.395e-001	1.584e+000
0.91400	9.985e-002	2.432e-001	1.571e+000
0.91800	9.938e-002	2.402e-001	1.540e+000
0.92200	1.007e-001	2.353e-001	1.560e+000
0.92600	1.008e-001	2.355e-001	1.531e+000
0.93000	9.991e-002	2.354e-001	1.497e+000
0.93400	9.814e-002	2.282e-001	1.536e+000
0.93800	9.601e-002	2.328e-001	1.556e+000
0.94200	9.628e-002	2.354e-001	1.502e+000
0.94600	9.539e-002	2.324e-001	1.516e+000
0.95000	9.316e-002	2.305e-001	1.520e+000
0.95400	9.565e-002	2.305e-001	1.504e+000

0.95800	9.241e-002	2.323e-001	1.514e+000
0.96200	8.905e-002	2.301e-001	1.491e+000
0.96600	9.176e-002	2.197e-001	1.532e+000
0.97000	8.850e-002	2.250e-001	1.507e+000
0.97400	9.139e-002	2.218e-001	1.493e+000
0.97800	8.766e-002	2.194e-001	1.463e+000
0.98200	8.475e-002	2.212e-001	1.452e+000
0.98600	8.674e-002	2.148e-001	1.477e+000
0.99000	8.578e-002	2.166e-001	1.452e+000
0.99400	8.232e-002	2.143e-001	1.467e+000
0.99800	8.639e-002	2.161e-001	1.460e+000
1.00200	8.237e-002	2.141e-001	1.425e+000
1.00600	8.476e-002	2.143e-001	1.479e+000
1.01000	8.514e-002	2.135e-001	1.467e+000
1.01400	8.305e-002	2.099e-001	1.414e+000
1.01800	8.273e-002	2.040e-001	1.435e+000
1.02200	7.922e-002	2.080e-001	1.410e+000
1.02600	7.989e-002	2.070e-001	1.417e+000
1.03000	7.852e-002	2.047e-001	1.405e+000
1.03400	7.788e-002	2.006e-001	1.411e+000
1.03800	7.818e-002	2.022e-001	1.397e+000
1.04200	7.693e-002	2.018e-001	1.413e+000
1.04600	7.561e-002	2.017e-001	1.391e+000
1.05000	7.681e-002	2.037e-001	1.403e+000
1.05400	7.683e-002	2.001e-001	1.406e+000
1.05800	7.521e-002	2.009e-001	1.407e+000
1.06200	7.480e-002	2.020e-001	1.364e+000
1.06600	7.436e-002	1.944e-001	1.391e+000
1.07000	7.115e-002	1.882e-001	1.391e+000
1.07400	7.426e-002	1.960e-001	1.372e+000
1.07800	7.100e-002	1.928e-001	1.410e+000

1.08200	7.377e-002	1.980e-001	1.388e+000
1.08600	7.037e-002	1.942e-001	1.354e+000
1.09000	7.147e-002	1.916e-001	1.353e+000
1.09400	7.058e-002	1.861e-001	1.343e+000
1.09800	7.020e-002	1.861e-001	1.338e+000
1.10200	7.091e-002	1.861e-001	1.354e+000
1.10600	6.981e-002	1.904e-001	1.348e+000
1.11000	6.806e-002	1.889e-001	1.356e+000
1.11400	6.606e-002	1.919e-001	1.320e+000
1.11800	6.753e-002	1.859e-001	1.328e+000
1.12200	6.768e-002	1.862e-001	1.309e+000
1.12600	6.647e-002	1.836e-001	1.304e+000
1.13000	6.581e-002	1.875e-001	1.290e+000
1.13400	6.617e-002	1.889e-001	1.278e+000
1.13800	6.463e-002	1.819e-001	1.310e+000
1.14200	6.212e-002	1.780e-001	1.324e+000
1.14600	6.460e-002	1.778e-001	1.292e+000
1.15000	6.393e-002	1.798e-001	1.279e+000
1.15400	6.245e-002	1.827e-001	1.287e+000
1.15800	6.137e-002	1.745e-001	1.303e+000
1.16200	6.154e-002	1.765e-001	1.302e+000
1.16600	6.209e-002	1.798e-001	1.282e+000
1.17000	5.996e-002	1.781e-001	1.316e+000
1.17400	5.973e-002	1.797e-001	1.278e+000
1.17800	5.899e-002	1.767e-001	1.278e+000
1.18200	5.970e-002	1.693e-001	1.272e+000
1.18600	5.904e-002	1.715e-001	1.288e+000
1.19000	5.763e-002	1.753e-001	1.273e+000
1.19400	5.804e-002	1.670e-001	1.284e+000
1.19800	5.740e-002	1.705e-001	1.263e+000
1.20200	5.797e-002	1.663e-001	1.280e+000

1.20600	5.764e-002	1.653e-001	1.281e+000
1.21000	5.505e-002	1.656e-001	1.253e+000
1.21400	5.774e-002	1.689e-001	1.285e+000
1.21800	5.472e-002	1.714e-001	1.266e+000
1.22200	5.375e-002	1.629e-001	1.247e+000
1.22600	5.449e-002	1.614e-001	1.249e+000
1.23000	5.484e-002	1.656e-001	1.274e+000
1.23400	5.508e-002	1.604e-001	1.243e+000
1.23800	5.416e-002	1.656e-001	1.255e+000
1.24200	5.310e-002	1.590e-001	1.234e+000
1.24600	5.236e-002	1.609e-001	1.221e+000
1.25000	5.308e-002	1.582e-001	1.220e+000
1.25400	5.337e-002	1.606e-001	1.207e+000
1.25800	5.223e-002	1.611e-001	1.227e+000
1.26200	5.165e-002	1.597e-001	1.230e+000
1.26600	5.186e-002	1.598e-001	1.205e+000
1.27000	5.168e-002	1.574e-001	1.206e+000
1.27400	5.006e-002	1.571e-001	1.213e+000
1.27800	5.149e-002	1.521e-001	1.198e+000
1.28200	5.025e-002	1.539e-001	1.203e+000
1.28600	5.116e-002	1.532e-001	1.202e+000
1.29000	5.018e-002	1.532e-001	1.187e+000
1.29400	4.921e-002	1.516e-001	1.168e+000
1.29800	4.841e-002	1.530e-001	1.170e+000
1.30200	4.953e-002	1.490e-001	1.156e+000
1.30600	4.764e-002	1.527e-001	1.140e+000
1.31000	4.715e-002	1.460e-001	1.153e+000
1.31400	4.880e-002	1.468e-001	1.166e+000
1.31800	4.728e-002	1.506e-001	1.142e+000
1.32200	4.654e-002	1.487e-001	1.130e+000
1.32600	4.782e-002	1.471e-001	1.121e+000

1.33000	4.730e-002	1.451e-001	1.158e+000
1.33400	4.724e-002	1.457e-001	1.160e+000
1.33800	4.578e-002	1.480e-001	1.140e+000
1.34200	4.591e-002	1.448e-001	1.127e+000
1.34600	4.513e-002	1.444e-001	1.155e+000
1.35000	4.458e-002	1.421e-001	1.131e+000
1.35400	4.509e-002	1.448e-001	1.107e+000
1.35800	4.357e-002	1.426e-001	1.077e+000
1.36200	4.451e-002	1.407e-001	1.129e+000
1.36600	4.420e-002	1.372e-001	1.095e+000
1.37000	4.283e-002	1.374e-001	1.117e+000
1.37400	4.430e-002	1.413e-001	1.105e+000
1.37800	4.367e-002	1.395e-001	1.097e+000
1.38200	4.297e-002	1.381e-001	1.102e+000
1.38600	4.370e-002	1.374e-001	1.108e+000
1.39000	4.282e-002	1.347e-001	1.075e+000
1.39400	3.993e-002	1.334e-001	1.099e+000
1.39800	4.182e-002	1.373e-001	1.110e+000
1.40200	4.142e-002	1.345e-001	1.085e+000
1.40600	4.124e-002	1.336e-001	1.061e+000
1.41000	4.141e-002	1.364e-001	1.106e+000
1.41400	4.169e-002	1.318e-001	1.075e+000
1.41800	4.150e-002	1.296e-001	1.085e+000
1.42200	4.091e-002	1.324e-001	1.057e+000
1.42600	4.092e-002	1.357e-001	1.067e+000
1.43000	3.847e-002	1.320e-001	1.064e+000
1.43400	3.959e-002	1.300e-001	1.078e+000
1.43800	3.918e-002	1.279e-001	1.074e+000
1.44200	4.079e-002	1.279e-001	1.053e+000
1.44600	3.817e-002	1.278e-001	1.062e+000
1.45000	3.774e-002	1.290e-001	1.059e+000

1.45400	3.745e-002	1.292e-001	1.074e+000
1.45800	3.789e-002	1.293e-001	1.037e+000
1.46200	3.653e-002	1.262e-001	1.053e+000
1.46600	3.678e-002	1.268e-001	1.020e+000
1.47000	3.800e-002	1.261e-001	1.049e+000
1.47400	3.888e-002	1.265e-001	1.065e+000
1.47800	3.662e-002	1.261e-001	1.077e+000
1.48200	3.666e-002	1.251e-001	1.044e+000
1.48600	3.693e-002	1.254e-001	1.039e+000
1.49000	3.584e-002	1.250e-001	1.012e+000
1.49400	3.585e-002	1.213e-001	1.032e+000
1.49800	3.565e-002	1.257e-001	1.010e+000
1.50200	3.506e-002	1.248e-001	9.912e-001
1.50600	3.619e-002	1.214e-001	1.022e+000
1.51000	3.563e-002	1.194e-001	1.017e+000
1.51400	3.537e-002	1.210e-001	1.009e+000
1.51800	3.471e-002	1.186e-001	1.042e+000
1.52200	3.488e-002	1.197e-001	9.999e-001
1.52600	3.542e-002	1.215e-001	1.019e+000
1.53000	3.404e-002	1.187e-001	1.006e+000
1.53400	3.421e-002	1.147e-001	9.697e-001
1.53800	3.429e-002	1.188e-001	9.847e-001
1.54200	3.445e-002	1.171e-001	9.633e-001
1.54600	3.452e-002	1.163e-001	9.855e-001
1.55000	3.390e-002	1.194e-001	9.606e-001
1.55400	3.342e-002	1.158e-001	9.638e-001
1.55800	3.271e-002	1.171e-001	9.675e-001
1.56200	3.308e-002	1.138e-001	9.705e-001
1.56600	3.219e-002	1.172e-001	9.674e-001
1.57000	3.345e-002	1.132e-001	9.645e-001
1.57400	3.280e-002	1.142e-001	9.869e-001

1.57800	3.178e-002	1.131e-001	9.853e-001
1.58200	3.177e-002	1.106e-001	9.672e-001
1.58600	3.248e-002	1.105e-001	9.987e-001
1.59000	3.176e-002	1.074e-001	9.653e-001
1.59400	3.120e-002	1.094e-001	9.703e-001
1.59800	3.093e-002	1.092e-001	9.459e-001
1.60200	3.103e-002	1.074e-001	9.681e-001
1.60600	3.136e-002	1.102e-001	9.593e-001
1.61000	3.019e-002	1.096e-001	9.599e-001
1.61400	3.048e-002	1.098e-001	9.415e-001
1.61800	3.045e-002	1.083e-001	9.422e-001
1.62200	3.064e-002	1.090e-001	9.520e-001
1.62600	3.013e-002	1.060e-001	9.665e-001
1.63000	3.010e-002	1.073e-001	9.285e-001
1.63400	2.920e-002	1.050e-001	9.335e-001
1.63800	2.896e-002	1.036e-001	9.246e-001
1.64200	2.845e-002	1.048e-001	9.083e-001
1.64600	2.921e-002	1.060e-001	9.165e-001
1.65000	2.960e-002	1.019e-001	9.140e-001
1.65400	2.940e-002	1.055e-001	9.336e-001
1.65800	2.897e-002	1.038e-001	9.346e-001
1.66200	2.900e-002	1.064e-001	9.222e-001
1.66600	2.880e-002	1.021e-001	8.952e-001
1.67000	2.898e-002	1.015e-001	9.103e-001
1.67400	2.846e-002	1.031e-001	9.075e-001
1.67800	2.793e-002	1.008e-001	9.126e-001
1.68200	2.794e-002	1.010e-001	9.333e-001
1.68600	2.871e-002	1.009e-001	9.377e-001
1.69000	2.757e-002	1.035e-001	9.236e-001
1.69400	2.772e-002	9.958e-002	9.242e-001
1.69800	2.830e-002	1.011e-001	9.141e-001

1.70200	2.778e-002	9.926e-002	9.126e-001
1.70600	2.718e-002	1.002e-001	9.141e-001
1.71000	2.727e-002	9.854e-002	8.773e-001
1.71400	2.743e-002	1.004e-001	8.996e-001
1.71800	2.754e-002	9.958e-002	8.947e-001
1.72200	2.651e-002	9.774e-002	8.935e-001
1.72600	2.709e-002	9.713e-002	8.980e-001
1.73000	2.740e-002	9.779e-002	8.960e-001
1.73400	2.619e-002	9.738e-002	8.960e-001
1.73800	2.574e-002	9.970e-002	8.850e-001
1.74200	2.589e-002	9.779e-002	8.752e-001
1.74600	2.578e-002	9.719e-002	8.653e-001
1.75000	2.621e-002	9.837e-002	8.586e-001
1.75400	2.505e-002	9.596e-002	8.632e-001
1.75800	2.511e-002	9.484e-002	8.594e-001
1.76200	2.526e-002	9.218e-002	8.700e-001
1.76600	2.533e-002	9.287e-002	8.848e-001
1.77000	2.510e-002	9.188e-002	8.345e-001
1.77400	2.443e-002	9.162e-002	8.375e-001
1.77800	2.424e-002	9.273e-002	8.498e-001
1.78200	2.453e-002	9.063e-002	8.571e-001
1.78600	2.423e-002	9.109e-002	8.315e-001
1.79000	2.461e-002	9.130e-002	8.352e-001
1.79400	2.435e-002	9.075e-002	8.373e-001
1.79800	2.393e-002	9.368e-002	8.165e-001
1.80200	2.361e-002	9.194e-002	8.211e-001
1.80600	2.326e-002	8.957e-002	8.399e-001
1.81000	2.344e-002	9.005e-002	8.283e-001
1.81400	2.305e-002	9.046e-002	8.141e-001
1.81800	2.305e-002	9.219e-002	8.186e-001
1.82200	2.347e-002	9.137e-002	8.061e-001

1.82600	2.240e-002	8.984e-002	8.225e-001
1.83000	2.325e-002	8.819e-002	8.142e-001
1.83400	2.304e-002	8.874e-002	8.173e-001
1.83800	2.282e-002	8.851e-002	8.040e-001
1.84200	2.211e-002	8.880e-002	8.136e-001
1.84600	2.235e-002	8.887e-002	8.113e-001
1.85000	2.267e-002	8.697e-002	7.904e-001
1.85400	2.239e-002	8.982e-002	8.067e-001
1.85800	2.220e-002	8.441e-002	8.050e-001
1.86200	2.224e-002	8.552e-002	7.766e-001
1.86600	2.220e-002	8.780e-002	8.033e-001
1.87000	2.203e-002	8.328e-002	7.764e-001
1.87400	2.179e-002	8.358e-002	7.936e-001
1.87800	2.112e-002	8.493e-002	7.881e-001
1.88200	2.149e-002	8.483e-002	7.916e-001
1.88600	2.115e-002	8.243e-002	7.801e-001
1.89000	2.134e-002	8.505e-002	7.762e-001
1.89400	2.098e-002	8.334e-002	8.052e-001
1.89800	2.112e-002	8.485e-002	7.695e-001
1.90200	2.102e-002	8.590e-002	7.959e-001
1.90600	2.102e-002	8.144e-002	7.935e-001
1.91000	2.123e-002	8.130e-002	8.004e-001
1.91400	2.063e-002	8.112e-002	7.917e-001
1.91800	2.030e-002	8.288e-002	8.077e-001
1.92200	2.030e-002	8.283e-002	7.689e-001
1.92600	1.998e-002	7.802e-002	7.843e-001
1.93000	2.004e-002	8.036e-002	7.687e-001
1.93400	1.987e-002	7.933e-002	7.879e-001
1.93800	1.969e-002	7.983e-002	7.820e-001
1.94200	1.954e-002	7.999e-002	7.842e-001
1.94600	2.005e-002	7.939e-002	7.596e-001

1.95000	2.003e-002	8.069e-002	7.645e-001
1.95400	1.983e-002	7.818e-002	7.591e-001
1.95800	1.941e-002	7.990e-002	7.731e-001
1.96200	1.965e-002	7.800e-002	7.609e-001
1.96600	1.914e-002	7.769e-002	7.356e-001
1.97000	1.981e-002	7.692e-002	7.429e-001
1.97400	1.940e-002	7.715e-002	7.413e-001
1.97800	1.925e-002	7.735e-002	7.275e-001
1.98200	1.879e-002	7.548e-002	7.394e-001
1.98600	1.941e-002	7.843e-002	7.298e-001
1.99000	1.859e-002	7.978e-002	7.367e-001
1.99400	1.888e-002	7.783e-002	7.327e-001
1.99800	1.894e-002	7.761e-002	7.373e-001
3.067e+002	4.206e+001	1.345e+001	2.00200

➢The code which used to generation photons (for abnormal blood)

Are same to code of normal just different in optical blood parameters

➢The output from monte carlo simulation (malaria blood)

number of photons = 10000.000000

bin size = 0.00400 [cm]

last row is overflow. Ignore.

r [cm]	Fsph [1/cm2]	Fcyl [1/cm2]	Fpla [1/cm2]
0.00200	1.839e+004	1.153e+002	4.090e+000
0.00600	2.079e+003	3.791e+001	2.806e+000
0.01000	7.707e+002	2.027e+001	2.388e+000
0.01400	3.565e+002	1.505e+001	2.006e+000
0.01800	2.256e+002	1.054e+001	1.804e+000

0.02200	1.483e+002	8.382e+000	1.652e+000
0.02600	1.013e+002	7.213e+000	1.459e+000
0.03000	6.783e+001	5.461e+000	1.301e+000
0.03400	6.002e+001	5.352e+000	1.157e+000
0.03800	4.480e+001	4.102e+000	1.166e+000
0.04200	3.648e+001	3.430e+000	1.061e+000
0.04600	2.988e+001	3.164e+000	9.481e-001
0.05000	2.313e+001	2.693e+000	9.363e-001
0.05400	2.057e+001	2.402e+000	9.325e-001
0.05800	1.792e+001	2.245e+000	8.224e-001
0.06200	1.550e+001	2.033e+000	8.117e-001
0.06600	1.199e+001	1.682e+000	6.578e-001
0.07000	1.140e+001	1.650e+000	6.455e-001
0.07400	1.015e+001	1.512e+000	5.622e-001
0.07800	7.747e+000	1.446e+000	5.816e-001
0.08200	7.366e+000	1.286e+000	5.517e-001
0.08600	6.229e+000	1.232e+000	5.996e-001
0.09000	6.080e+000	1.110e+000	5.286e-001
0.09400	5.135e+000	9.910e-001	4.838e-001
0.09800	4.311e+000	9.547e-001	4.574e-001
0.10200	3.938e+000	8.385e-001	4.454e-001
0.10600	3.731e+000	8.104e-001	4.126e-001
0.11000	3.313e+000	7.431e-001	4.377e-001
0.11400	3.232e+000	7.159e-001	4.010e-001
0.11800	2.669e+000	6.531e-001	3.798e-001
0.12200	2.746e+000	6.364e-001	3.500e-001
0.12600	2.406e+000	6.001e-001	3.446e-001
0.13000	2.180e+000	5.193e-001	3.182e-001
0.13400	2.147e+000	4.988e-001	3.259e-001
0.13800	1.797e+000	4.353e-001	2.939e-001
0.14200	1.784e+000	5.105e-001	2.880e-001

0.14600	1.571e+000	4.596e-001	2.886e-001
0.15000	1.476e+000	3.877e-001	2.681e-001
0.15400	1.352e+000	3.963e-001	2.474e-001
0.15800	1.200e+000	3.525e-001	2.229e-001
0.16200	1.262e+000	3.660e-001	2.104e-001
0.16600	1.020e+000	3.163e-001	2.417e-001
0.17000	8.702e-001	3.007e-001	2.233e-001
0.17400	9.533e-001	2.823e-001	1.870e-001
0.17800	8.633e-001	2.953e-001	2.000e-001
0.18200	8.602e-001	2.869e-001	1.784e-001
0.18600	6.905e-001	2.410e-001	1.944e-001
0.19000	7.671e-001	2.539e-001	1.864e-001
0.19400	7.313e-001	2.271e-001	1.677e-001
0.19800	6.140e-001	1.814e-001	1.549e-001
0.20200	5.823e-001	2.082e-001	1.602e-001
0.20600	5.506e-001	1.968e-001	1.422e-001
0.21000	5.168e-001	1.561e-001	1.606e-001
0.21400	4.746e-001	1.816e-001	1.520e-001
0.21800	4.951e-001	1.798e-001	1.341e-001
0.22200	4.623e-001	1.692e-001	1.393e-001
0.22600	4.466e-001	1.803e-001	1.214e-001
0.23000	3.802e-001	1.345e-001	1.342e-001
0.23400	2.883e-001	1.229e-001	1.116e-001
0.23800	3.419e-001	1.355e-001	1.116e-001
0.24200	2.862e-001	1.218e-001	1.081e-001
0.24600	3.542e-001	1.159e-001	1.065e-001
0.25000	2.510e-001	1.201e-001	9.499e-002
0.25400	2.925e-001	9.748e-002	1.138e-001
0.25800	2.809e-001	1.104e-001	1.008e-001
0.26200	2.113e-001	9.353e-002	8.760e-002
0.26600	2.398e-001	8.347e-002	7.338e-002

0.27000	2.194e-001	8.493e-002	8.367e-002
0.27400	2.151e-001	9.118e-002	6.895e-002
0.27800	1.886e-001	8.809e-002	7.254e-002
0.28200	1.997e-001	6.764e-002	8.754e-002
0.28600	2.004e-001	7.989e-002	7.719e-002
0.29000	1.595e-001	6.576e-002	6.943e-002
0.29400	1.512e-001	7.031e-002	7.507e-002
0.29800	1.334e-001	6.702e-002	6.983e-002
0.30200	1.490e-001	5.806e-002	5.973e-002
0.30600	1.302e-001	6.747e-002	5.517e-002
0.31000	1.260e-001	6.382e-002	6.916e-002
0.31400	1.504e-001	5.453e-002	5.540e-002
0.31800	1.224e-001	5.667e-002	5.525e-002
0.32200	9.147e-002	5.020e-002	6.818e-002
0.32600	1.163e-001	4.613e-002	4.100e-002
0.33000	9.955e-002	4.092e-002	4.927e-002
0.33400	8.243e-002	4.522e-002	4.806e-002
0.33800	7.004e-002	3.817e-002	5.086e-002
0.34200	8.136e-002	4.462e-002	4.994e-002
0.34600	7.777e-002	3.616e-002	4.675e-002
0.35000	7.773e-002	3.850e-002	3.950e-002
0.35400	7.399e-002	3.739e-002	4.358e-002
0.35800	7.586e-002	3.891e-002	3.670e-002
0.36200	6.379e-002	3.776e-002	3.098e-002
0.36600	6.879e-002	2.913e-002	3.765e-002
0.37000	6.358e-002	3.024e-002	3.710e-002
0.37400	5.671e-002	3.205e-002	3.628e-002
0.37800	6.268e-002	3.649e-002	4.029e-002
0.38200	5.962e-002	3.325e-002	3.107e-002
0.38600	5.239e-002	2.394e-002	2.748e-002
0.39000	5.258e-002	2.281e-002	2.679e-002

0.39400	5.535e-002	2.499e-002	3.063e-002
0.39800	4.152e-002	2.046e-002	3.424e-002
0.40200	3.734e-002	2.185e-002	2.294e-002
0.40600	4.390e-002	2.599e-002	2.727e-002
0.41000	4.386e-002	2.483e-002	2.325e-002
0.41400	3.497e-002	2.086e-002	2.411e-002
0.41800	4.277e-002	2.339e-002	2.466e-002
0.42200	3.945e-002	2.175e-002	2.259e-002
0.42600	3.202e-002	1.540e-002	2.733e-002
0.43000	3.251e-002	2.166e-002	2.329e-002
0.43400	3.235e-002	1.870e-002	2.084e-002
0.43800	2.708e-002	1.929e-002	2.319e-002
0.44200	3.100e-002	1.682e-002	1.786e-002
0.44600	2.972e-002	1.617e-002	1.678e-002
0.45000	2.733e-002	1.569e-002	2.106e-002
0.45400	2.343e-002	1.576e-002	2.410e-002
0.45800	2.514e-002	1.554e-002	1.988e-002
0.46200	2.539e-002	1.602e-002	2.198e-002
0.46600	2.134e-002	1.306e-002	1.731e-002
0.47000	1.982e-002	1.451e-002	1.576e-002
0.47400	2.168e-002	1.221e-002	1.408e-002
0.47800	2.136e-002	1.329e-002	1.298e-002
0.48200	2.229e-002	1.223e-002	1.730e-002
0.48600	2.057e-002	1.349e-002	1.405e-002
0.49000	1.562e-002	9.614e-003	1.932e-002
0.49400	1.507e-002	1.061e-002	1.931e-002
0.49800	1.925e-002	8.797e-003	1.167e-002
0.50200	1.559e-002	7.415e-003	1.276e-002
0.50600	1.461e-002	8.227e-003	9.304e-003
0.51000	1.292e-002	9.643e-003	1.216e-002
0.51400	1.520e-002	8.939e-003	1.253e-002

0.51800	1.408e-002	7.739e-003	1.188e-002
0.52200	1.231e-002	7.526e-003	1.126e-002
0.52600	1.078e-002	7.384e-003	1.172e-002
0.53000	1.346e-002	7.651e-003	1.243e-002
0.53400	1.191e-002	7.213e-003	8.456e-003
0.53800	1.137e-002	7.156e-003	1.071e-002
0.54200	9.610e-003	7.778e-003	1.026e-002
0.54600	9.679e-003	6.771e-003	7.518e-003
0.55000	9.417e-003	6.440e-003	8.095e-003
0.55400	1.093e-002	6.384e-003	1.447e-002
0.55800	1.144e-002	6.006e-003	6.867e-003
0.56200	9.446e-003	4.654e-003	8.225e-003
0.56600	7.590e-003	5.343e-003	8.982e-003
0.57000	8.426e-003	5.506e-003	6.875e-003
0.57400	7.276e-003	4.678e-003	4.965e-003
0.57800	7.027e-003	5.523e-003	6.762e-003
0.58200	7.869e-003	4.609e-003	6.582e-003
0.58600	7.036e-003	7.195e-003	9.515e-003
0.59000	6.616e-003	4.844e-003	8.479e-003
0.59400	8.057e-003	5.243e-003	6.322e-003
0.59800	6.287e-003	3.593e-003	4.394e-003
0.60200	7.242e-003	4.933e-003	3.507e-003
0.60600	6.549e-003	3.934e-003	5.564e-003
0.61000	6.971e-003	4.318e-003	4.581e-003
0.61400	5.394e-003	2.672e-003	4.809e-003
0.61800	5.481e-003	3.445e-003	4.006e-003
0.62200	4.919e-003	3.367e-003	4.487e-003
0.62600	4.877e-003	3.482e-003	4.471e-003
0.63000	4.229e-003	1.878e-003	3.428e-003
0.63400	4.736e-003	2.603e-003	7.167e-003
0.63800	3.451e-003	2.390e-003	3.636e-003

0.64200	3.128e-003	3.614e-003	3.567e-003
0.64600	3.593e-003	3.460e-003	2.595e-003
0.65000	3.573e-003	3.266e-003	3.973e-003
0.65400	5.155e-003	2.765e-003	3.958e-003
0.65800	3.642e-003	2.136e-003	1.739e-003
0.66200	3.936e-003	3.170e-003	4.676e-003
0.66600	3.068e-003	2.513e-003	2.832e-003
0.67000	3.239e-003	2.458e-003	4.559e-003
0.67400	2.651e-003	2.497e-003	3.162e-003
0.67800	3.026e-003	1.762e-003	3.887e-003
0.68200	2.863e-003	1.661e-003	3.439e-003
0.68600	3.896e-003	1.835e-003	3.097e-003
0.69000	1.850e-003	2.218e-003	3.771e-003
0.69400	2.492e-003	1.746e-003	3.921e-003
0.69800	2.328e-003	1.471e-003	2.122e-003
0.70200	2.743e-003	1.953e-003	2.491e-003
0.70600	1.686e-003	1.554e-003	5.012e-003
0.71000	2.930e-003	1.672e-003	3.103e-003
0.71400	1.734e-003	2.147e-003	2.177e-003
0.71800	1.718e-003	1.796e-003	2.041e-003
0.72200	2.211e-003	1.405e-003	2.015e-003
0.72600	1.505e-003	1.621e-003	2.375e-003
0.73000	2.633e-003	1.808e-003	4.498e-003
0.73400	1.789e-003	1.605e-003	1.949e-003
0.73800	2.367e-003	1.475e-003	2.115e-003
0.74200	1.414e-003	1.539e-003	2.465e-003
0.74600	1.592e-003	8.853e-004	2.499e-003
0.75000	1.260e-003	1.431e-003	1.433e-003
0.75400	9.894e-004	1.211e-003	2.106e-003
0.75800	1.278e-003	9.335e-004	2.752e-003
0.76200	1.266e-003	8.431e-004	2.547e-003

0.76600	9.846e-004	1.092e-003	1.667e-003
0.77000	1.556e-003	7.436e-004	1.411e-003
0.77400	1.442e-003	8.372e-004	1.539e-003
0.77800	1.012e-003	4.934e-004	1.370e-003
0.78200	1.115e-003	7.469e-004	5.967e-004
0.78600	9.031e-004	6.520e-004	1.326e-003
0.79000	1.244e-003	1.038e-003	1.741e-003
0.79400	1.163e-003	1.051e-003	1.291e-003
0.79800	9.797e-004	8.463e-004	1.525e-003
0.80200	8.873e-004	5.179e-004	2.103e-003
0.80600	8.912e-004	6.689e-004	1.623e-003
0.81000	8.546e-004	4.609e-004	1.742e-003
0.81400	8.975e-004	7.237e-004	1.255e-003
0.81800	6.643e-004	9.768e-004	1.599e-003
0.82200	6.732e-004	1.053e-003	1.272e-003
0.82600	7.678e-004	6.676e-004	1.508e-003
0.83000	7.718e-004	4.837e-004	7.638e-004
0.83400	6.934e-004	8.008e-004	1.322e-003
0.83800	6.742e-004	6.963e-004	2.122e-003
0.84200	7.090e-004	6.664e-004	1.222e-003
0.84600	9.235e-004	3.407e-004	6.882e-004
0.85000	6.961e-004	5.310e-004	2.094e-003
0.85400	4.084e-004	4.061e-004	4.904e-004
0.85800	5.803e-004	5.534e-004	1.206e-003
0.86200	5.116e-004	4.968e-004	6.055e-004
0.86600	8.532e-004	4.651e-004	1.065e-003
0.87000	6.908e-004	3.311e-004	2.726e-004
0.87400	5.716e-004	3.613e-004	1.566e-003
0.87800	4.839e-004	2.705e-004	2.724e-004
0.88200	3.027e-004	2.769e-004	4.675e-004
0.88600	3.948e-004	2.694e-004	4.844e-004

0.89000	4.438e-004	4.602e-004	1.782e-003
0.89400	6.585e-004	3.991e-004	7.070e-004
0.89800	3.228e-004	4.178e-004	4.319e-004
0.90200	4.248e-004	2.388e-004	7.871e-004
0.90600	4.042e-004	2.347e-004	8.757e-004
0.91000	3.945e-004	3.488e-004	6.438e-004
0.91400	4.603e-004	3.703e-004	4.844e-004
0.91800	4.015e-004	2.673e-004	2.789e-004
0.92200	4.148e-004	6.488e-004	6.225e-004
0.92600	2.668e-004	3.394e-004	8.212e-004
0.93000	2.762e-004	1.818e-004	4.845e-004
0.93400	2.827e-004	2.574e-004	5.728e-004
0.93800	2.683e-004	2.491e-004	3.246e-004
0.94200	2.601e-004	2.309e-004	2.232e-004
0.94600	2.167e-004	3.939e-004	2.727e-004
0.95000	3.046e-004	1.618e-004	2.641e-004
0.95400	2.101e-004	3.173e-004	1.173e-003
0.95800	2.393e-004	1.248e-004	4.733e-004
0.96200	2.332e-004	1.851e-004	5.697e-004
0.96600	2.394e-004	3.306e-004	2.793e-004
0.97000	2.761e-004	2.932e-004	2.685e-004
0.97400	3.286e-004	2.164e-004	4.547e-005
0.97800	1.581e-004	2.652e-004	1.793e-004
0.98200	2.431e-004	2.654e-004	1.450e-004
0.98600	3.485e-004	1.603e-004	4.864e-004
0.99000	1.201e-004	2.211e-004	3.996e-004
0.99400	2.803e-004	2.100e-004	1.991e-004
0.99800	2.007e-004	1.590e-004	3.099e-004
1.00200	2.104e-004	2.859e-004	5.519e-004
1.00600	2.328e-004	2.110e-004	1.404e-004
1.01000	2.279e-004	2.347e-004	2.511e-004

1.01400	2.492e-004	1.941e-004	4.812e-004
1.01800	1.092e-004	3.038e-004	5.641e-004
1.02200	1.498e-004	1.838e-004	4.336e-005
1.02600	2.164e-004	1.216e-004	2.532e-004
1.03000	1.713e-004	6.546e-005	5.223e-004
1.03400	1.647e-004	9.945e-005	0.000e+000
1.03800	6.091e-005	2.175e-004	6.018e-004
1.04200	1.725e-004	1.723e-004	0.000e+000
1.04600	1.722e-004	2.779e-004	1.837e-004
1.05000	1.289e-004	1.690e-004	9.953e-005
1.05400	1.326e-004	1.013e-004	9.094e-005
1.05800	1.238e-004	2.238e-004	8.883e-005
1.06200	8.096e-005	1.457e-004	3.736e-004
1.06600	9.852e-005	9.425e-005	5.202e-004
1.07000	1.055e-004	4.443e-005	8.682e-005
1.07400	1.130e-004	1.097e-004	9.094e-005
1.07800	1.293e-004	1.293e-004	1.339e-004
1.08200	3.588e-005	1.246e-004	0.000e+000
1.08600	1.635e-004	6.151e-005	4.365e-004
1.09000	7.804e-005	5.315e-005	0.000e+000
1.09400	6.303e-005	7.561e-005	1.884e-004
1.09800	6.948e-005	8.148e-005	4.711e-004
1.10200	7.875e-005	9.919e-005	1.322e-004
1.10600	7.146e-005	1.312e-004	0.000e+000
1.11000	1.552e-004	6.823e-005	3.460e-004
1.11400	1.152e-004	9.956e-005	9.953e-005
1.11800	4.489e-005	1.100e-004	4.336e-005
1.12200	4.771e-005	1.272e-004	0.000e+000
1.12600	6.231e-005	9.000e-005	4.336e-005
1.13000	1.079e-004	1.231e-004	1.383e-004
1.13400	3.899e-005	3.742e-005	9.094e-005

1.13800	3.501e-005	2.154e-004	0.000e+000
1.14200	5.396e-005	8.716e-005	6.012e-004
1.14600	8.302e-005	6.444e-005	4.380e-004
1.15000	4.770e-005	2.755e-005	1.450e-004
1.15400	6.047e-005	5.765e-005	4.547e-005
1.15800	5.198e-005	7.270e-005	4.547e-005
1.16200	5.094e-005	9.861e-005	4.910e-004
1.16600	6.422e-005	3.806e-005	0.000e+000
1.17000	6.190e-005	1.125e-005	4.547e-005
1.17400	4.520e-005	1.765e-005	9.491e-005
1.17800	4.590e-005	6.012e-005	8.883e-005
1.18200	8.617e-005	3.612e-005	2.511e-004
1.18600	6.770e-005	6.149e-005	4.547e-005
1.19000	2.106e-005	2.778e-005	8.471e-005
1.19400	5.492e-005	7.621e-005	0.000e+000
1.19800	3.187e-005	3.791e-005	4.547e-005
1.20200	4.332e-005	5.015e-005	9.094e-005
1.20600	3.797e-005	9.859e-005	0.000e+000
1.21000	4.184e-005	2.909e-005	0.000e+000
1.21400	4.997e-005	2.469e-005	4.336e-005
1.21800	5.434e-005	1.781e-005	0.000e+000
1.22200	4.826e-005	3.765e-005	0.000e+000
1.22600	2.990e-005	1.320e-004	1.404e-004
1.23000	3.914e-005	3.917e-005	9.491e-005
1.23400	6.226e-005	3.396e-005	0.000e+000
1.23800	3.539e-005	3.964e-005	0.000e+000
1.24200	4.034e-005	1.086e-005	0.000e+000
1.24600	6.884e-006	4.608e-005	0.000e+000
1.25000	1.639e-005	5.597e-005	0.000e+000
1.25400	3.565e-005	2.364e-005	0.000e+000
1.25800	2.703e-005	5.232e-006	0.000e+000

1.26200	1.135e-005	0.000e+000	1.383e-004
1.26600	2.735e-005	8.412e-005	0.000e+000
1.27000	2.695e-005	3.672e-005	4.336e-005
1.27400	1.568e-005	6.050e-005	4.336e-005
1.27800	3.046e-005	2.288e-005	0.000e+000
1.28200	2.526e-005	8.279e-005	0.000e+000
1.28600	2.561e-005	2.249e-005	0.000e+000
1.29000	1.057e-005	1.631e-005	0.000e+000
1.29400	2.679e-005	5.086e-006	0.000e+000
1.29800	1.062e-005	2.203e-005	0.000e+000
1.30200	1.939e-005	1.160e-005	0.000e+000
1.30600	4.721e-005	3.590e-005	0.000e+000
1.31000	3.928e-006	1.632e-005	0.000e+000
1.31400	2.499e-005	3.487e-005	0.000e+000
1.31800	6.642e-006	0.000e+000	1.898e-004
1.32200	8.577e-006	3.908e-005	8.631e-005
1.32600	1.136e-005	3.560e-005	4.336e-005
1.33000	5.274e-005	2.766e-005	0.000e+000
1.33400	1.547e-005	0.000e+000	0.000e+000
1.33800	3.004e-005	8.483e-005	9.051e-005
1.34200	2.285e-005	5.393e-006	0.000e+000
1.34600	1.997e-006	1.070e-005	0.000e+000
1.35000	1.199e-005	5.028e-005	0.000e+000
1.35400	1.434e-005	0.000e+000	4.336e-005
1.35800	2.628e-005	1.675e-005	0.000e+000
1.36200	1.860e-006	1.492e-005	0.000e+000
1.36600	1.925e-005	1.106e-005	0.000e+000
1.37000	1.686e-005	2.205e-005	0.000e+000
1.37400	5.661e-006	1.527e-005	0.000e+000
1.37800	1.168e-005	4.555e-006	4.336e-005
1.38200	1.732e-005	5.237e-006	8.673e-005

1.38600	9.768e-006	9.728e-006	0.000e+000
1.39000	1.034e-005	2.765e-005	1.981e-004
1.39400	2.511e-005	2.170e-005	4.135e-005
1.39800	9.832e-006	2.151e-005	0.000e+000
1.40200	1.756e-006	0.000e+000	0.000e+000
1.40600	0.000e+000	0.000e+000	0.000e+000
1.41000	9.518e-006	3.022e-005	0.000e+000
1.41400	7.071e-006	9.761e-006	0.000e+000
1.41800	1.716e-006	0.000e+000	0.000e+000
1.42200	2.042e-005	1.114e-005	0.000e+000
1.42600	0.000e+000	1.521e-005	0.000e+000
1.43000	3.539e-006	0.000e+000	0.000e+000
1.43400	8.889e-006	0.000e+000	0.000e+000
1.43800	4.778e-006	0.000e+000	0.000e+000
1.44200	1.200e-005	4.786e-006	0.000e+000
1.44600	1.300e-005	1.497e-005	0.000e+000
1.45000	1.721e-006	0.000e+000	0.000e+000
1.45400	1.649e-005	4.746e-006	0.000e+000
1.45800	0.000e+000	4.305e-006	0.000e+000
1.46200	4.682e-006	4.721e-006	0.000e+000
1.46600	6.658e-006	4.937e-006	9.051e-005
1.47000	6.453e-006	2.359e-005	0.000e+000
1.47400	4.842e-006	0.000e+000	0.000e+000
1.47800	3.458e-006	1.022e-005	4.135e-005
1.48200	1.210e-005	4.883e-006	0.000e+000
1.48600	1.563e-006	4.644e-006	0.000e+000
1.49000	3.037e-006	0.000e+000	2.077e-004
1.49400	7.407e-006	0.000e+000	0.000e+000
1.49800	0.000e+000	0.000e+000	0.000e+000
1.50200	7.999e-006	1.488e-005	9.491e-005
1.50600	8.042e-006	0.000e+000	0.000e+000

1.51000	0.000e+000	0.000e+000	0.000e+000
1.51400	0.000e+000	0.000e+000	0.000e+000
1.51800	2.995e-006	4.546e-006	0.000e+000
1.52200	7.484e-006	0.000e+000	0.000e+000
1.52600	0.000e+000	1.374e-005	0.000e+000
1.53000	1.546e-006	0.000e+000	0.000e+000
1.53400	1.334e-006	0.000e+000	0.000e+000
1.53800	4.372e-006	4.487e-006	0.000e+000
1.54200	1.384e-006	2.472e-005	0.000e+000
1.54600	2.891e-006	0.000e+000	0.000e+000
1.55000	1.436e-006	0.000e+000	0.000e+000
1.55400	2.844e-006	4.235e-006	0.000e+000
1.55800	0.000e+000	0.000e+000	0.000e+000
1.56200	0.000e+000	0.000e+000	0.000e+000
1.56600	1.407e-006	0.000e+000	0.000e+000
1.57000	0.000e+000	1.009e-005	0.000e+000
1.57400	6.363e-006	4.598e-006	0.000e+000
1.57800	0.000e+000	4.586e-006	0.000e+000
1.58200	0.000e+000	0.000e+000	0.000e+000
1.58600	0.000e+000	0.000e+000	4.336e-005
1.59000	4.032e-006	0.000e+000	0.000e+000
1.59400	1.424e-006	0.000e+000	0.000e+000
1.59800	4.309e-006	4.319e-006	0.000e+000
1.60200	0.000e+000	0.000e+000	0.000e+000
1.60600	2.928e-006	0.000e+000	0.000e+000
1.61000	0.000e+000	0.000e+000	0.000e+000
1.61400	0.000e+000	0.000e+000	0.000e+000
1.61800	5.452e-006	4.265e-006	0.000e+000
1.62200	0.000e+000	0.000e+000	0.000e+000
1.62600	0.000e+000	0.000e+000	0.000e+000
1.63000	0.000e+000	0.000e+000	0.000e+000

1.63400	0.000e+000	0.000e+000	0.000e+000
1.63800	1.226e-006	0.000e+000	0.000e+000
1.64200	0.000e+000	3.198e-005	0.000e+000
1.64600	0.000e+000	0.000e+000	0.000e+000
1.65000	2.646e-006	0.000e+000	0.000e+000
1.65400	2.761e-006	1.784e-005	0.000e+000
1.65800	0.000e+000	9.554e-006	0.000e+000
1.66200	1.249e-006	4.152e-006	0.000e+000
1.66600	0.000e+000	0.000e+000	0.000e+000
1.67000	1.180e-006	0.000e+000	0.000e+000
1.67400	0.000e+000	8.605e-006	0.000e+000
1.67800	2.558e-006	3.922e-006	0.000e+000
1.68200	1.163e-006	3.913e-006	0.000e+000
1.68600	0.000e+000	0.000e+000	0.000e+000
1.69000	0.000e+000	0.000e+000	0.000e+000
1.69400	0.000e+000	0.000e+000	0.000e+000
1.69800	0.000e+000	0.000e+000	0.000e+000
1.70200	0.000e+000	0.000e+000	3.943e-005
1.70600	0.000e+000	0.000e+000	0.000e+000
1.71000	0.000e+000	0.000e+000	0.000e+000
1.71400	2.696e-006	4.222e-006	0.000e+000
1.71800	2.440e-006	0.000e+000	0.000e+000
1.72200	2.219e-006	0.000e+000	0.000e+000
1.72600	0.000e+000	0.000e+000	0.000e+000
1.73000	1.153e-006	0.000e+000	0.000e+000
1.73400	1.044e-006	1.907e-005	0.000e+000
1.73800	0.000e+000	4.164e-006	0.000e+000
1.74200	1.192e-006	0.000e+000	0.000e+000
1.74600	2.598e-006	0.000e+000	0.000e+000
1.75000	1.075e-006	2.284e-005	0.000e+000
1.75400	6.550e-006	1.219e-005	0.000e+000

1.75800	5.349e-006	0.000e+000	0.000e+000
1.76200	1.111e-006	3.735e-006	0.000e+000
1.76600	0.000e+000	0.000e+000	0.000e+000
1.77000	0.000e+000	0.000e+000	0.000e+000
1.77400	6.159e-006	0.000e+000	0.000e+000
1.77800	3.382e-006	0.000e+000	0.000e+000
1.78200	0.000e+000	0.000e+000	0.000e+000
1.78600	0.000e+000	1.765e-005	0.000e+000
1.79000	2.248e-006	8.439e-006	0.000e+000
1.79400	0.000e+000	0.000e+000	0.000e+000
1.79800	8.280e-006	0.000e+000	0.000e+000
1.80200	0.000e+000	0.000e+000	0.000e+000
1.80600	0.000e+000	0.000e+000	0.000e+000
1.81000	0.000e+000	0.000e+000	0.000e+000
1.81400	0.000e+000	0.000e+000	0.000e+000
1.81800	0.000e+000	0.000e+000	0.000e+000
1.82200	0.000e+000	0.000e+000	0.000e+000
1.82600	0.000e+000	0.000e+000	0.000e+000
1.83000	0.000e+000	0.000e+000	0.000e+000
1.83400	0.000e+000	3.763e-006	0.000e+000
1.83800	0.000e+000	0.000e+000	0.000e+000
1.84200	1.017e-006	3.747e-006	0.000e+000
1.84600	0.000e+000	0.000e+000	0.000e+000
1.85000	0.000e+000	0.000e+000	0.000e+000
1.85400	0.000e+000	0.000e+000	0.000e+000
1.85800	0.000e+000	0.000e+000	0.000e+000
1.86200	0.000e+000	0.000e+000	0.000e+000
1.86600	0.000e+000	0.000e+000	0.000e+000
1.87000	0.000e+000	0.000e+000	0.000e+000
1.87400	9.826e-007	0.000e+000	0.000e+000
1.87800	0.000e+000	0.000e+000	0.000e+000

1.88200	0.000e+000	0.000e+000	0.000e+000
1.88600	0.000e+000	0.000e+000	0.000e+000
1.89000	0.000e+000	7.622e-006	0.000e+000
1.89400	0.000e+000	0.000e+000	0.000e+000
1.89800	0.000e+000	0.000e+000	0.000e+000
1.90200	1.991e-006	0.000e+000	0.000e+000
1.90600	0.000e+000	3.453e-006	0.000e+000
1.91000	9.020e-007	0.000e+000	0.000e+000
1.91400	0.000e+000	0.000e+000	0.000e+000
1.91800	8.945e-007	0.000e+000	0.000e+000
1.92200	0.000e+000	0.000e+000	0.000e+000
1.92600	0.000e+000	0.000e+000	0.000e+000
1.93000	0.000e+000	0.000e+000	0.000e+000
1.93400	0.000e+000	0.000e+000	0.000e+000
1.93800	0.000e+000	0.000e+000	0.000e+000
1.94200	0.000e+000	0.000e+000	0.000e+000
1.94600	0.000e+000	0.000e+000	0.000e+000
1.95000	0.000e+000	0.000e+000	0.000e+000
1.95400	0.000e+000	0.000e+000	0.000e+000
1.95800	0.000e+000	0.000e+000	0.000e+000
1.96200	0.000e+000	0.000e+000	0.000e+000
1.96600	0.000e+000	0.000e+000	0.000e+000
1.97000	0.000e+000	0.000e+000	0.000e+000
1.97400	0.000e+000	0.000e+000	0.000e+000
1.97800	0.000e+000	0.000e+000	0.000e+000
1.98200	0.000e+000	0.000e+000	0.000e+000
1.98600	0.000e+000	0.000e+000	0.000e+000
1.99000	0.000e+000	0.000e+000	0.000e+000
1.99400	0.000e+000	0.000e+000	0.000e+000
1.99800	0.000e+000	0.000e+000	0.000e+000
2.00200	0.000e+000	0.000e+000	0.000e+000